OPTIMIZATION AND DESIGN OF UNDERGROUND EMBEDDED PENSTOCKS

SOUREN B. HADJIAN

MAJOR TECHNICAL REPORT
IN
THE DEPARTMENT
OF
CIVIL ENGINEERING

PRESENTED IN PARTIAL FULFILLMENT OF THE
REQUIREMENT FOR THE DEGREE OF MASTER
OF ENGINEERING
AT
CONCORDIA UNIVERSITY
MONTREAL QUEBEC CANADA

FEBRUARY 1980

RESUME

OPTIMISATION ET CONCEPTION D'UNE CONDUITE FORCEE SOUTERRAINE

SOUREN HADJIAN

Le but de ce rapport est de recueillir les renseignements nécessaires à une étude d'optimisation économique d'une conduite forcée telle qu'utilisée dans un projet hydro-électrique.

Ce rapport traite d'abord de l'analyse théorique de l'aspect hydraulique d'une conduite. Il en aborde ensuite l'analyse et le design structural. Ces deux facteurs sont ensuite combinés en tenant compte des coûts de l'investissement, tels les coûts de perte de charge et les coûts de construction (matériaux et main-d'oeuvre).

Cette étude considère aussi l'influence de la nature du roc ainsi que de sa consolidation.

De plus, ce rapport contient un organigramme montrant les étapes à suivre pour une optimisation manuelle ou par ordinateur.

ABSTRACT

OPTIMIZATION AND DESIGN OF UNDERGROUND EMBEDDED PENSTOCKS

SOUREN HADJIAN

The intent of this report is to act as a guide in the optimization and design of underground embedded penstocks of hydroelectric projects.

The report presents hydraulic background of the penstock and treats the structural design of the wall of the penstock, known as the penstock liner.

These hydraulic and structural design factors are inter-related by their common influence on the total cost of the project.

The optimization considers among other things the cost of construction which includes excavation, concreting and consolidation of rock surrounding the penstocks. The price of energy is also reflected in the optimization through the hydraulic head losses.

Finally a flow chart is presented to enable the engineer to optimize the design of a penstock either manually or by the use of a computer.

ACKNOWLEDGEMENTS

The author wishes to express his gratitude to his supervisor, Dr. O.A. Pekau Eng. of Concordia University for his guidance in the realisation of this report.

Special thanks to Mr. Joe Raffaele Eng. for making suggestions towards improvement of the presentation. The author is also gratefull to Mr. Guy Grenier, Eng. and his collegues at Rousseau, Sauvé, Warren Inc. for their help and encouragement.

The typing of the manuscript by Miss Lise Emond and the assistance in preparation of the figures by Mr. Edmond Amar are gratefully acknowledged.

TABLE OF CONTENTS

LIST OF FIGURES

LIST OF SYMBOLS

Symbols are defined where they first appear in the text. Those symbols which appear often in the text are defined below.

A_w = area of cross section of weld

D = diameter of the penstock

d = root opening for welding

E = Young's modulus

e = joint efficiency

f = friction factor

f'_c = strength of concrete

f_y = yield strength of steel

g = gravitational acceleration

H_o = piezometric head over the steel liner

H_r = thickness of rock cover

h = hydrostatic head

h_b = head loss due to bend

h_c = head loss due to contraction

h_f = head loss due to friction

h_r = rock thickness above the penstock

k_b = experimental loss coefficient for bend

k = $\frac{D}{t}$ in buckling formulas for the steel liner

L = length of the oil coated section

l = length of the conduit

M = bending moment

P = external hydrostatic pressure

P_{cr} = collapse pressure

R = internal radius of the liner

R_b = radius of curvature of an elbow

R_e = Reynold's number

S = circumferential design stress

S_p = tensile stress due to temperature change

S_t = tensile stress due to Poisson's effect

T = total rise of a steep slope of rock

t = thickness of the liner

U = indent in the steel liner

v = average velocity of flow in the penstock

y_o = initial gap between the steel liner and the surrounding concrete

α = angle of convergence

β = correction factor for experimental bend coefficients

γ = specific weight of water

ΔT = difference in temperature

δ = elongation

ε = rugosity

εT = thermal expansion

θ = angle of inclination

λ = average value of friction factor in a reducer

ν = poisson's ratio

ν_k = kinematic viscosity

σ_n = unit stress in steel liner

σ_3 = confining pressure in rock

CHAPTER I

INTRODUCTION

1.1 General

In a hydroelectric project one of the aims of the design is to convey water from the reservoir to the turbines as efficiently as possible. This is done by the use of conduits called penstocks.

The purpose of this report is to give guidelines to design safe, hydraulically efficient and economically feasible underground embedded penstocks.

The importance of the study of a penstock is manifested by its cost which could be as high as 20% of the total investment of the structures in a hydroelectric project (excluding cost of the dams and dykes).

Optimization includes the engineering study (structural, hydraulic, geotechnical) of the penstock diameter, its location and its path of the flow, combined with an assessment of its cost as part of the total monetary investment in the project.

1.2 Types of Penstocks

The types of penstocks are characterized by their position with respect to the terrain, i.e. underground or surface, and by their building materials, i.e. concrete, steel or just excavated tunnel in rock.

Underground embedded penstocks are those that are excavated in rock and then are lined either with concrete or with steel. These types of penstocks are preferred to surface penstocks where climate is severe or

where terrain is rugged with steep depressions, provided that an adequate rock cover and rock quality are available. Flexibility of routing the penstocks in the case of underground penstocks is advantageous compared to surface penstocks where geometry is constrained by surface topography. In contrast, where rock is not sound and fault zones are encountered embedded penstocks can be very expensive to build. Thus it necessary conduct a collective overall study of the cost of the items of one type of penstock and compare it with the cost of the other type to determine the most economical design.

1.3. Parts of a Common Type of Penstock

A penstock can have many parts, depending on type of dam, location of the intake structure, the outlet works and powerhouse. Figure 1 illustrates a profile of a common type of underground embedded penstock for an earthfill dam with a surface powerhouse. In the figure the penstock has five sections; they are the upper and the lower elbows, the inclined section, the horizontal section and the reducer. The upper elbow is attached to the transition as shown in figure 2. The transition which is a part of the water intake structure funnels water from the reservoir to the upper elbow of the penstock. The downstream end of the penstock is fitted to the scroll case by a make-up piece as shown in figure 3. The scroll case is a spiral tube that diminishes in size while feeding the blades of the turbine with water through multiple openings.

1.4 Organization of the Report

The report presents the hydraulic and structural background required for the design of a penstock. It also deals with possible geotechnical problems associated with the rock surrounding the penstock and discusses remedial measures for such problems. Further, the report explains the important role of the angle of inclination in the total economy of the penstock. The optimization process for the angle of inclination and penstock diameter is discussed using a flowchart as an illustrative guideline. Finally, a numerical example is solved to illustrate the important factors discussed.

CHAPTER II

HYDRAULIC ANALYSIS OF A PENSTOCK

2.1 Introduction

With the rapid escalation of the cost of energy hydraulic losses are of paramount importance in the optimization of a penstock. A proper assessment of these losses enables the designer to establish an optimum diameter of a penstock from the hydraulic point of view.

Penstocks are analysed as closed pipes flowing full. Data from laboratory tests are often not applicable since these tests are conducted on small pipes which are not necessarily representative of the penstocks which may possess very large diameters. However, studies such as those of United States Bureau of Reclamation (USBR) (1, 2, 3) which are based on observations of actual hydroplants can be safely used.

2.2 Hydraulic Losses in a Penstock

The hydraulic design of a penstock is aimed mainly at the reduction of losses over the life of a project and affects the overall economy of the project.

There are two types of losses. Friction losses which are the result of the wall roughness of the penstock and secondary losses which are caused by trashracks*, slots for the water intake structure gates, the shape of the water entrance, bends in the penstock and reduction in size of the

---

* A trashrack is a metal grid installed at the mouth of the water intake structure to prevent debris from entering a penstock.

penstock (contraction). Of the secondary losses only those due to bends and contractions will be discussed. The other losses are usually associated with the design of the water intake structure.

2.2.1 Friction Losses

Friction losses which account for most of the head losses in a penstock are calculated by the Darcy and Weisbach formula (4, 5, 6)

$$h_f = f \frac{l}{D} \frac{v^2}{2g} \qquad (2.1)$$

Where: h_f = drop in hydraulic grade line or friction loss;

f = friction factor;

l = length of the conduit;

D = diameter of the conduit;

v = mean velocity of flow;

g = gravitational acceleration.

The friction factor, f, is a function of Reynolds number, Re, which is given by:

$$Re = \frac{Dv}{\nu_k} \qquad (2.2)$$

Where: ν_k = kinematic viscosity

Values of ν_k which is a function of the water temperature are given in chart 1 in appendix A.

The friction factor is also a function of the surface roughness of the wall of the penstock. The wall roughness is called rugosity which is usually expressed as relative rugosity:

$$\text{Relative rugosity} = \frac{\varepsilon}{D} \qquad (2.3)$$

Where: ε = rugosity.

Rugosity for different surfaces compiled by Brater and King (6) are tabulated in table 1 in appendix A.

2.1.1.1 Reynolds Number and Types of FLow

The state of flow in a penstock is determined by its Reynolds number. The magnitude of Reynolds number characterizes flow to be laminar, turbulent or in a zone in between called transitional flow.

The flow is laminar if the Reynolds number of the flow is less than 2 000. The relationship between the Reynolds number and the friction factor for a laminar flow is given by:

$$f = \frac{64}{Re} \qquad (2.4)$$

Turbulent flow has a Reynolds number larger than 4 000. With Reynolds number within the range of 2 000 to 4 000 the flow could be either laminar or turbulent. Because of this uncertainty it is the practice to assume turbulent flow in this zone. This leads to a diameter larger than that assuming laminar flow, thus ensuring the efficiency of the system.

Having the kinematic viscosity and the velocity of a penstock a set of trial diameters are entered into equation 2.2 which gives corresponding Reynolds numbers. With these Reynolds numbers friction factors of each

diameter can be found from Moody's diagram. (chart 2 in appendix A) Using equation 2.1, losses can be determined with the friction factors. As an example the relationship between diameter and head loss due to friction is studied for a discharge of 240 m/sec, viscosity of water at 35°C, rugosity of concrete wall 0.6 mm. The results of the studies conducted on 5 diameters of 5.0, 5.5, 6.0, 6.5 and 7.0 m penstocks are plotted in figure 4. It is evident that the larger the diameter the less is the head loss due to friction.

2.2.2 Secondary Losses

The percentage of minor losses compared to the overall losses could be small in long penstocks. However, for short penstocks the term secondary losses could be misleading since their magnitude could match or exceed that of the friction losses in which case the secondary losses could be a major determinant factor in the optimization process. Bends and contractions are the most common sources of secondary losses in penstocks.

a) Bends

Bends or elbows dissipate part of the kinetic energy of water. Losses are given by:

$$h_b = k_b \frac{v^2}{2g} \qquad (2.5)$$

Where: h_b = head loss due to bend;

k_b = experimental loss coefficient.

Values for k provided by many authors (1,2) are shown in chart 3 in appendix A. These k values are results of experiments performed on pipes having diameters ranging from 3 cm to 20 cm. Therefore, these values can only be confidently applied to small diameter conduits and it could be erroneous to use them for large penstocks. Reliable k values are given by Levin (5) in chart 4 in appendix A. Levin's values for k_b are given as functions of $\frac{\varepsilon}{D}$ (relative rugosity), angle of curvature of the bend and radius of curvature, R_b. Although chart 4 is limited to penstocks with $\frac{R_b}{D} = 10$ and $Re > 2 \times 10^5$, k_b values for ratios other than $\frac{R_b}{D}=10$ can be found by applying a correction factor β to k_b values. In chart 5, appendix A correction factor β can be found which is a function of $\frac{R_b}{D}$ and Reynolds number. k_b found in chart 4, appendix A for ratios of $\frac{R_b}{D}=10$, is then multiplied by the factor β.

b) Contractions

Contractions or reducers are those portions of a penstock over which the diameter is reduced as shown in figure 5. The change in diameter is recommended where lining material is changed from concrete to steel. Since a steel liner has a smoother wall surface the head loss in the steel lined section is considerably less than that of the concrete. This permits the reduction of the diameter without affecting the head loss. Contraction losses are given by (5):

$$h_c = \frac{\lambda}{8 \sin \frac{\alpha}{2}} \cdot \frac{\delta^2 - 1}{\delta^2} \cdot \frac{v_I^2}{2g} \qquad (2.6)$$

Where: λ = average value of the friction factor for the large and the small sections;

α = angle of convergence of the cone which is a function of the length L over which the contraction takes place;

$\delta = \frac{S2}{S1}$ ratio of the large to the small section, (figure 5) ;

v_1 = average velocity in the smaller section.

Where it is economical the reducer can be incorporated with the lower elbow. Figure 6 shows a horizontal reducer and one incorporated with the lower elbow.

CHAPTER III

STRUCTURAL AND GEOTECHNICAL ANALYSIS OF A PENSTOCK

3.1 General

Although rock around a penstock can be consolidated by grouting, some hairline cracks which are difficult to seal will remain. High pressure water which infiltrates into these cracks in the surrounding rock from the penstocks might cause hydraulic jacking and create tensile cracks in the solid rock surrounding a penstock. These tensile cracks could impair the stability of the rock above the penstock. Hydraulic jacking or fracturing occurs when the confining pressure in rock is overcome by interstitial water pressure such that:

$$\gamma h > \sigma_3$$

Where: σ_3 = confining pressure;

h = head of water, measured between the reservoir level and the elevation of the penstock;

γ = specific weight of water.

Confining pressure exerted by the weight of rock is low where rock cover above a penstock is shallow. It is also low in fractured rock that exists either in that state or is damaged by blasting in the vicinity.

Depending on the ratio of confining pressure to water pressure, rock stability could be assured either by lining the penstock with steel and filling the space between the rock and the steel liner with concrete or by a concrete lining.

Design of the penstock liner includes the choice of lining material (steel or concrete), the determining of its thickness and establishing the length of the steel liner where steel lining is essential. The design also considers the necessity for consolidating the rock surrounding the penstock.

3.2 Loads on the Penstock Liner

The two principal loadings on a penstock liner are the internal and external water pressure. The case of simultaneous occurence of the two pressures is ignored since it will have negligible effect on the liner. Both pressures are taken as the head due to the difference in elevation between the maximum reservoir level and the elevation of the lowest part of the penstock. Figure 7 shows two penstock sections one with internal pressure and the other with external pressure.

The internal pressure is constant throughout the horizontal section of the penstock. Its magnitude is augmented by a factor in order to account for the water hammer effect (7). This factor which is a function of the time of the closure of the gates at the turbine, the length and diameter of the penstock, the static head and the velocity of flow is determined by an independent analysis.

The external pressure on the other hand diminishes towards the downstream end of the liner. There, water is exposed to atmospheric pressure. The external pressure is developed on the liner of an empty penstock when water seeps from adjacent pressurized penstock or from the reservoir through fissures in the rock mass.

3.3 Design of a Concrete Liner

A load sharing exists between the concrete and the surrounding rock under internal pressure. Tests have shown that 30% of the pressure is carried by the liner and the rest by the rock (8). Thus, the external pressure is the dominating load in the determination of the thickness of the concrete liner.

The following formulae describe the resistance of liner concrete against the circumferencial or hoop compressive stress due to external pressure:

$$P\,(R + t_{max}) = .85\, f'_c\,(t_{min} - \rho) \qquad (3.2)$$

and

$$P\,(R + t_{av.}) = \frac{.85\, f'_c}{1.25}\,(t_{av.} - \rho) \qquad (3.3)$$

Where: t_{min} = minimum design thickness, no overbreak or rock is considered, cm;

t_{max} = t_{min} + 25, 25 is the overbreak in cm;

$t_{av.}$ = average thickness of the liner: t_{min} + 12, cm;

R. = internal radius of the liner, cm;

f'_c = specified compressive strength of concrete, MPa;

1.25 = safety factor;

P = external hydrostatic pressure, MPa;

ρ = tolerence for minimum and average thickness of the liner, cm.

Both formulae are based on the ultimate resistance of concrete in compression. Equation 3.2 does not carry a load factor because the exter-

nal pressure is well defined, i.e. the level of water in the reservoir cannot be higher than the maximum, since any excess will flow out of the reservoir by the spillway. The presentation of the thickness in the formula is such that any possible variation in the overbreak can only result in a more conservative value of the thickness. But in equation 3.3 a load factor of 1.25 is introduced in order to account for the unfavourable variation in the average thickness.

Because the concrete liner is almost always designed for external pressure, i.e. for compression loads, it is not reinforced by steel except at the interface between the concrete lined section and the steel lined section and that is done only to control shrinkage and to distribute anchorage stresses. Figure 8 shows a section through a typical concrete lined penstock.

3.4 Design of a Steel Liner

An annular space between the steel liner and the embedment concrete might form because of difference in temperature between the concrete and the water in the penstock. Temperature drop of water will shrink the liner and open a gap. This gap could be increased by creep in rock. That is, rock could creep with time under the internal pressure from the penstock and when the penstock is emptied the steel liner which is still in elastic state will retain its original shape while rock and concrete will remain as they were. Because of existence of this gap, rock around the steel lined section is not relied upon to share loads with the steel section.

Therefore, under internal pressure the thickness of the liner is controlled by hoop stress:

$$\sigma_n = \frac{PD}{2et}$$

Where: σ_n = unit stress, MPa;

P = internal pressure, MPa;

D = internal diameter, cm;

e = joint efficiency taken as 95% (.95);

t = wall thickness of the steel liner, cm.

For the external pressure Timoshenko's theory of elastic buckling cannot be employed since it does not consider any confinement around the liner (9). Under external pressure, failure could occur when the hoop stress reaches the yield stress of the steel (fy). This relation is given by:

$$P_{cr} = \frac{2f_y t}{D} \qquad (3.5)$$

Where: P_{cr} = critical external pressure or collapse pressure.

However, the liner might collapse due to elastic instability before yield stress is reached. This phenomenon is studied by Vaughan (10), Borot (11), Montel (12) and Amstutz (13).

Vaughan and Borot assume that failure of the steel liner will occur by buckling in an even number of waves around the circumference as shown in figure 9. The collapse pressure P_{cr} according to this assumption is given by the following relation:

$$\frac{13k^2}{4E'} P_{cr}^2 + 2P_{cr}\left(1 + 3k\frac{y_o}{R} - \frac{f_y k}{2E'}\right) - \left(\frac{4f_y}{k} - \frac{f_y^2}{E'}\right) = 0 \qquad (3.6)$$

Where: y_o = initial gap between the liner and the concrete, cm;

R = internal radius of the liner, cm;

$E' = \frac{E}{\sqrt{1-\nu^2}}$;

E = young's modulus, MPa;

ν = poisson's ratio;

k = D/t

Montel analyses liners with initial imperfections, i.e. liners with some flatness which can occur either during transportation or during handling and assemblage. Figure 10 shows this imperfection on the circumference of the liner. The semi-empirical formula that takes into account these imperfections (indents) is given by:

$$P_{cr} = \frac{14.14\ f_y}{(k)^{3/2}\left\{1 + 1.2\ \frac{U + 2y_o}{t}\right\}} \qquad (3.7)$$

Where: U = initial imperfection cm.

Montel recommends the use of his formula in the range of $0.1t < U < 5t$.

Another approach is taken by Amstuts where in his research he assumes that buckling will occur forming one single lobe rather than multiple waves as considered by Vaughan and Borot; figure 11 illustrates this assumption showing the new mean radius generating a mean curve about which two outward and one inward half waves are formed. This behaviour is expressed by the following two equations:

$$\left(\frac{f_n}{E'} + \frac{y_o}{R}\right)\left[1 + \frac{3k^2 f_n}{E'}\right]^{3/2} = 1.68k\ \frac{f'_y - f_n}{E'}\left[1 - \frac{k(f'_y - f_n)}{4E'}\right] \qquad (3.8)$$

and

$$\left(1 - \frac{P_{cr}\,k}{2f_n}\right) = 0.175\ \frac{k}{E'}\ (f'_y - f_n) \qquad (3.9)$$

Where: $f'_y = \frac{f_y}{\sqrt{1-\nu-\nu^2}}$

f_n = theoretical compressive stress, MPa;

Upon solving equations 3.8 and 3.9 simultaneously, f_n and P_{cr} can be determined.

To assess which of the foregoing hypotheses is closest to reality "Société des Forges et Ateliers du Creusot" (14) conducted tests on behalf of Electricité du France on liners with 4 000 mm diameter and thicknesses ranging from 12 mm to 24 mm. The results of these tests are plotted on a graph as collapse pressure, P_{cr}, against the ratios $k = \frac{D}{t}$ (figure 12). On the same diagram, results obtained from equations of Vaughan - Borot, Montel as well as Amstutz using similar values as the test are plotted. Amstutz's curve estimates collapse pressure lower than the critical pressure from the tests and therefore is conservative.

However, in order to include the effect of initial imperfections as studied by Montel, Amstutz's curve instead of being independent of the values of indents may be drawn parallel to Montel's curve as shown in figure 13.

Apart from the internal and external pressures there are other loads on the penstocks that can cause important longitudinal stresses on the liner. These stresses are caused by:

a) Temperature changes

Rock temperature remains constant while seasons change. However water temperature in the reservoir changes. The difference in temperature between the steel liner and the surrounding rock results in the following stress:

$$S_t = E \cdot \varepsilon T \cdot \Delta T \qquad (3.10)$$

Where: S_t = tensile stress due to temperature change, MPa;

E = modulus of elasticity, MPa;

εT = coefficient of expansion;

ΔT = difference in temperature, ^oF.

b) Poisson's effect

Internal pressure that expands the liner radially will shrink it longitudinally. The opposite effect is true in case of the application of external pressure. This is called Poisson's effect. Since the liner is usually restrained against movement by stiffener rings, the change in circumference of the liner will cause compressive stresses in case of the external pressure and tensile stresses in case of the internal pressure. These stresses can be evaluated by using Poisson's ratio as follows:

$$S_p < 0.3\ S \qquad (3.11)$$

Where: S_p = stress due to Poisson's effect, MPa;

0.3 = Poisson's ratio for steel;

S = allowable circumferential design stress, MPa.

c) Stresses in the Steel Liner due to Shrinkage of Weld

Welding will not add any longitudinal stresses if the steel liner is not restrained against movement. Therefore it is recommended to have all the weldings performed before embedding the liner. If this is not possible as in the case of the transition between the scroll case and the penstock, the outside surface of liner should be coated with oil before concreting. Shrinkafe of a butt-weld can be evaluated by :(15)

$$\delta = 0.2 \left(\frac{A_w}{t}\right) + .05d \qquad (3.12)$$

Where: δ = transverse weld shrinkage, cm;

A_w = area of cross section of weld, cm^2;

t = thickness of steel liner, cm;

d = root opening, cm.

Longitudinal stresses in the steel liner can be calculated from the strain caused by the shrinkage of the weld δ.

d) Bending at Coated Section

Absence of cohesion between an oil coated steel liner and embedment concrete could cause the steel liner to bend longitudinally under partial loading as shown in figure 14. The bending moment at the centre of the coated section which augments longitudinal stresses in the liner is derived from the bending theory of axisymmetrically loaded cylindrical shells (16), (appendix B)

$$M_{max} = \frac{P}{2\beta^2} e^{-(\beta L/2)} \cdot \sin(\beta L/2) \qquad (3.13)$$

Where: $\beta = \sqrt[4]{\frac{3(1-\nu^2)}{R^2t^2}}$;

L = length of the coated section.

3.5 Length of the Steel Liner

To locate where $\sigma_3 > \gamma h$, i.e. where the liner is no longer needed, finite element analysis could be used. But for all practical purposes the empirical formulae derived by Terzaghi (17) and Olsen (18) are simpler to use.

Terzaghi suggests that any penstock with gentle sloping rock cover as shown in figure 15 having rock thickness less than half the hydrostatic head should be steel lined, i.e.:

$$\frac{h}{2} > h_r \qquad (3.14)$$

Where: h_r = rock thickness above the penstock cm.

Olsen on the other hand, upon studying steeper slopes concludes that a steel liner should be provided up to where:

$$H_r > \frac{H_o^2}{2T} + 50 \qquad (3.15)$$

Where: H_r = thickness of rock perpendicular to the average slope of the surface of rock cm;

T = total rise of the steep slope cm;

H_o = piezometric head over the steel liner cm.

3.6 Grouting

Grouting is the process of pumping a mixture of water and cement or a mixture of water, cement and sand into fissures in the rock mass or in voids left between the concrete and rock during placement of concrete or due to subsequent shrinkage. The grout is pumped through injection holes that intersect the assumed pattern of rock joints.

The cost of grouting around a penstock is a parameter in the optimization of the penstock. The cost of grouting is directly proportional to the length of the penstock.

There are many types of grouting each serving a specific purpose. The following types of grouting could be involved in the construction of a penstock:

a) Void Grouting

The purpose of void grouting is to fill voids created by entrapped air during placement of concrete either in the concrete lined section or in the encasement concrete in the steel lined section. Voids could also be left due to impossibility of placing concrete, particularly at the crown.

b) Consolidation Grouting

This type of grouting is performed to consolidate damaged rock around the penstock due to excavation blasting. Consolidation grouting can be carried deep into the rock to inject fissures created by relaxed rock or other naturally occuring joints and fissures. Consolidation improves the deformation modulus of the concrete liner. It also reduces the possibility of cracking of the rock when the penstock is pressurized.

c) Embedment Grouting

Embedment grouting is performed to seal the gap between the steel liner and the surrounding encasement concrete. The gap is formed by shrinkage of the concrete and by the shrinkage of the steel liner due to the temperature difference between the rock mass and the flowing water in the penstock.

d) Contact Grouting

This process is similar to embedment grouting but the gap to seal in this case is between the concrete and the surrounding rock. The

contact grouting pressure should not exceed the design collapse pressure for the steel liner.

CHAPTER IV

LENGTH OF THE PENSTOCK

4.1 General

The positions of the water intake structure and the powerhouse apart from their dependence on the position of the dam are influenced by the topography of the terrain. Their positions are also controlled by the balancing of the excavated material from construction of the powerhouse with the required fill material for construction of the dams and dykes. However, the relative position of the powerhouse with respect to position of the water intake structure is a function of the length of the penstock between them. A long penstock is disadvantageous because of its costly construction and because in some cases where penstocks exceed a certain length the use of surge tanks is unavoidable (19). The limiting value for the length of penstocks such that no surge tank is required, is a function of the time of closure of the wicket gates of the turbines and the subsequent water hammer in the penstock. Current practice shows that for penstocks shorter than 400 m surge tanks are rarely needed.

After the positions of the intake structure and powerhouse have been finalized, it is economically important to find the optimum path for the penstock between them within the practical construction limitations. The aim of this study is to optimize the path of the penstock between the water intake structure and the powerhouse.

4.2 Optimization of the Path of the Penstocks

The path of the penstock is a function of the positions of the water intake structure and the powerhouse. The intent of the optimization

is to keep the overall cost as low as possible. This can be achieved by providing the shortest possible penstock with restrictions imposed by economical construction procedures.

Although the shortest path gives the minimum volume of excavation and concrete, for the use of practical and economical construction procedures the angle of the inclined section of the penstock should not be less than 45^{o} to the horizontal. An inclination angle greater than the minimum, provides a slope that facilitates the disposal of the excavated material by self-mucking, i.e. the excavated material would flow freely down the slope to be collected downstream, thus avoiding costly mechanical removal of the excavated material. Steep inclination angles result in longer penstocks with longer bends, with consequent higher friction losses and higher bend losses. Therefore, it is recommended to keep the angle of inclination of a penstock between 45^{o} and 60^{o} provided that the distance and difference in elevation between the powerhouse and the intake structure can accommodate such angles.

4.3 Other Considerations

A distance of 4 to 5 diameters is needed between the end of the lower elbow and the entrance of the scroll case to permit the water to attain uniform flow conditions prior to its entrance into the scroll case.

For maintenance a penstock may need complete dewatering. To avoid ponding in the horizontal section a slope of 0.5% is provided to drain water in a sump downstream.

CHAPTER V

OPTIMIZATION PROCEDURE

5.1 General

The process of optimization blends the hydraulic, structural and geotechnical data by virtue of the fact that they all have effect on the total cost of construction of a penstock.

The economic study of the current market prices of each item is essential to the optimization of a penstock. The prices of items considered are: price of excavation per unit volume, price of concrete per unit volume, price of energy expressed as cost per unit length of head loss and price of grouting per unit length of penstock.

5.2 Process of Optimization

The aim of the optimization is to select the angle of inclination and the diameters of the concrete and steel lined sections which will give the most economical arrangement of the penstock.

The fixed parameters in the optimization are the head of water in the reservoir, the discharge, the horizontal projected length of the penstock and the physical properties of the construction materials. The rest of the parameters are variable and are functions of inclination angle or the diameters D_1 and D_2, the diameters of the concrete and steel lined sections respectively, as discussed in the hydraulic and structural studies.

To optimize the angle of the inclination two diameters are assigned for the concrete and the steel lined sections. Since, the inclination angle is not sensitive to the diameter, a preliminary calculation using

the hydraulic data can provide two diameters sufficient for the purpose of optimization of the angle of inclination. The process of iteration consists of varying the angle of inclination over the range 45 to 90 degrees keeping the diameters constant. The process involves the calculation of the thicknesses of both the concrete and steel liners by equations 3.2, 3.3, 3.8 and 3.9 with the length of the steel liner obtained from an independent geotechnical study. The quantities of excavation and construction materials such as steel and concrete as well as grouting quantities are calculated for each cycle of the iteration. Concurrent with each cycle of iteration the energy losses in terms of head loss due to friction, bends and contractions are calculated. For each cycle, the above quantities are calculated in terms of monetary investment. The total cost of the penstocks is calculated for each cycle after which the optimum slope is chosen.

The optimization of the diameters D_1 and D_2 follows, keeping the optimum angle obtained above constant. The iteration process varies them by the method of steepest descent. For each variation, i.e. for each assigned value for D_1 and D_2 the thicknesses of both the steel and concrete sections are calculated. This is followed by the calculations of their quantities and the losses due to friction, bends and contractions. The total cost for each cycle is then calculated. The iteration stops when the least costing penstock is found. The steps of the optimization are shown in the flowchart in figure 17.

5.3 Numerical Example

For illustration a numerical example is solved. The values used are based on a study of the 1980 market prices (20). The physical properties are as follows:

- Discharge — 300 m^3/sec
- Installed capacity — 300 MW
- Total head — 120 m
- Horizontal projected length of liner — 280 m
- Length of steel liner — 50 m
- Internal pressure with 25% rise due to water hammer — 1.5 MPa
- Rugosity
  - concrete — 4.6×10^{-5} m
  - steel — 6.1×10^{-4} m
- Steel used — G40.21 300 W
- Concrete f'_c — 30 MPa

Costs of items are as follows:

- Upper elbow
  - excavation — \$ 40/m^3
  - concreting — \$355/m^3
- Inclined section (55^o to 70^o)
  - excavation — \$115/m^3
  - concreting — \$400/m^3
- Vertical section (90^o)
  - excavation — \$105/m^3
  - concreting — \$365/m^3

- Lower elbow (55^{o} to 70^{o})
  - excavation $ 85/m^3
  - concreting $565/$m^3$
- Lower elbow (90^{o})
  - excavation $ 90/m^3
  - concreting $665/$m^3$
- Horizontal section (concrete liner)
  - excavation $ 65/m^3
  - concreting $350/$m^3$
- Horizontal section (steel liner)
  - excavation $ 65/m^3
  - concreting $150/$m^3$
  - steel lining $2.4/kg
- Reducer
  - excavation $ 65/m^3
  - concreting
    - if concrete lined $470/$m^3$
    - if steel lined $150/$m^3$
  - steel lining $3.3/kg
- Cost of energy expressed as $ per unit head loss 13.2×10^{6}/m
- Cost of grouting expressed as dollars per unit length of the penstock $200/m

With these values the optimum angle of inclination can be chosen. The relation between the angle of inclination to total cost is plotted in figure 18. The quantities of excavation and concrete are plotted in figures 19 and 20 respectively. The head losses for D_1 and D_2 are plotted in figure 21. When the costs of all these items are summed; D_1 and D_2 are expressed as functions of the total cost of construction. The matrix on figure 22 forms a concave upward surface with the optimum combination of D_1 and D_2 forming the point of stationary having the least costing penstock of 5.95 million dollars for D_1 = 7.00m and D_2 = 7.90m.

CHAPTER VI

CONCLUSION

While some papers and textbooks treat some parts of the subject of design of penstocks, specific detailed design information covering all the elements of a penstock is not available.

The aim of the report was to assemble the theoretical information required for the optimization of the design of a penstock. The influence and application of the following factors involved in the optimization process were discussed in detail:

- Hydraulic losses caused by friction, bends and contractions;
- Structural theories and formulas for calculation of the thicknesses of the wall of the penstock to withstand the exerted pressures;
- Treatment of shattered rock around a penstock;
- Construction factors which influence the routing arrangement;
- Investment in terms of construction and energy.

The optimization procedure presented shows how this information can be used in a systematic fashion to design a penstock which will have the minimum total cost while satisfying all of the constraints imposed by the project.

The method of optimization was illustrated by a solved example using an actual design of a penstock with discussions of the solution and results.

REFERENCES

(1) Bier, P.O. "Welded Steel Penstocks", Engineering Monograph No 3, Bureau of Reclamation, Denver, Colorado, 1967.

(2) Bradley, J.N., and Thompson, L.R., "Friction Factors for Large Conduits Flowing Full", Engineering Monograph No 7, Bureau of Reclamation, Denver, Colorado, 1965.

(3) Arthur, H.G., and Hilf, J.W., "Design of Gravity Dams", Bureau of Reclamation, Denver, Colorado, 1976.

(4) Streeter, Victor L., "Fluid Mechanics", McGraw-Hill, Book Co. Ltd, New-York, 1974.

(5) Levin, L., "Formulaire des conduites forcées, oléoducs et conduits d'aération", Dunod, Paris, 1968.

(6) Brater, Ernest F., and King, Horace Williams, "Handbook of Hydraulic for the Solution of Hydraulic Engineering Problems", McGraw-Hill Book Co., Ltd, New-York, 1976.

(7) Parmakian, John, "Waterhammer Analysis", Dover Publications, Inc., Now-York, 1963.

(8) Birkland, Halvard W., "The Widson of the Structure", ACI, Proceedings, V.75, No. 4, April, 1978, pp. 105-111.

(9) Timoshenko, Stephen P., and Gere, James M., "Theory of Elastic Stability", McGraw-Hill Book Co. Inc, New-York, 1961.

(10) Vaughan, E.W., "Steel Linings for Pressure Shafts in Solid Rock", Proceedings of the American Society of Civil Engineers, Pow Devision Roc., Paper 948, April 1956.

(11) Borot, H., "Buckling of a Thin Walled Tube Fitted in a Rigid Outer Covering and Subjected to an External Pressure", La Houille Blanche, No. 6, December, 1957, pp. 881-887.

(12) Montel, R., "A Semi-Empirical Formula for Determining the Limiting External Pressure for the Collapse of Smooth Metal Pipes Embedded in Concrete", La Houille Blanche, No. 5, September 1960, pp. 560-568.

(13) Amstutz, Ernst, "Einbeulen von Vorgespannten Schacht und Stollen Panzerungen", Schweizerische Bauzeitung, April 1953.

(14) "Bossellement d'une virole enrobée de béton", Société des Forges et Atelier du Creusot, Usines Schneider, internal document, 1963.

(15) Linnert, George E., "Welding Metallurgy", American Welding Society, Vol. 2, New York, 1965.

(16) Timoshenko, Stephen, and Woinowsky-Krieger, S., "Theory of Plates and Shells", McGraw-Hill Book Co. Inc., New-York, 1959.

(17) Terzaghi, karl, "Stability of Steep Slopes on Hard Unweathered Rock", Géotechnique, Vol. 12, No 3, pp. 199-208.

(18) Olsen, R. Selmer, "Influence des Zones Argileuses sur la Nécessité de Recouvrir la Roche à Haute Pression interne d'Eau ou d'Air", Report No 7, Ingeniorgeologi, Norges Tekniske Hogskole, Trondheim.

(19) Davis, Calvin V., and Sorenson, Kenneth E., "Handbook of Applied Hydraulics", McGraw-Hill Book Co. Inc., New-York, 1969.

(20) "Conduites Forcées, Optimization des Diamétres et de la Pente", Rousseau, Sauvé, Warren Inc., internal document, Montreal, 1978.

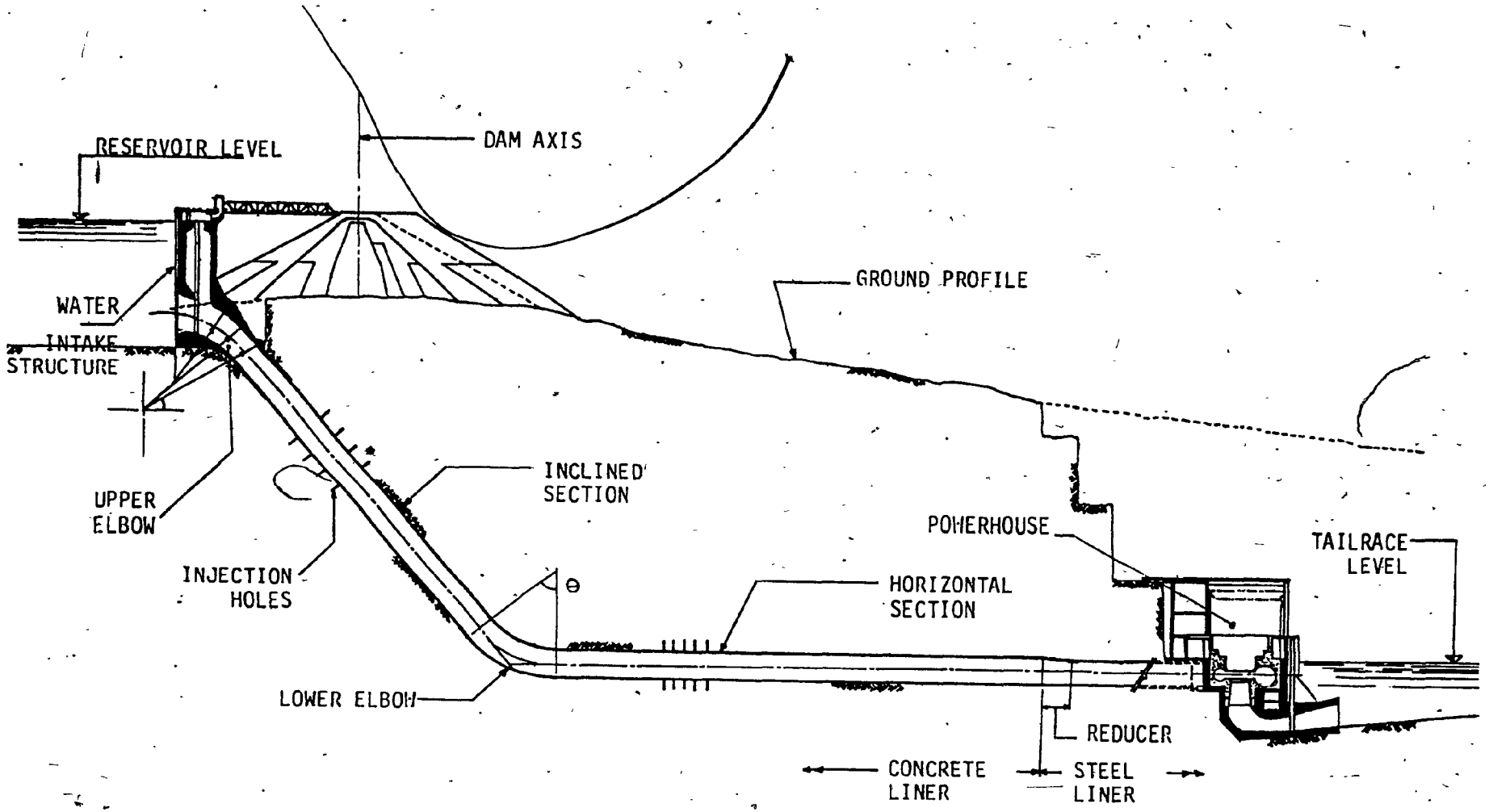

FIGURE 1.- Profile of a common type of embedded underground penstock.

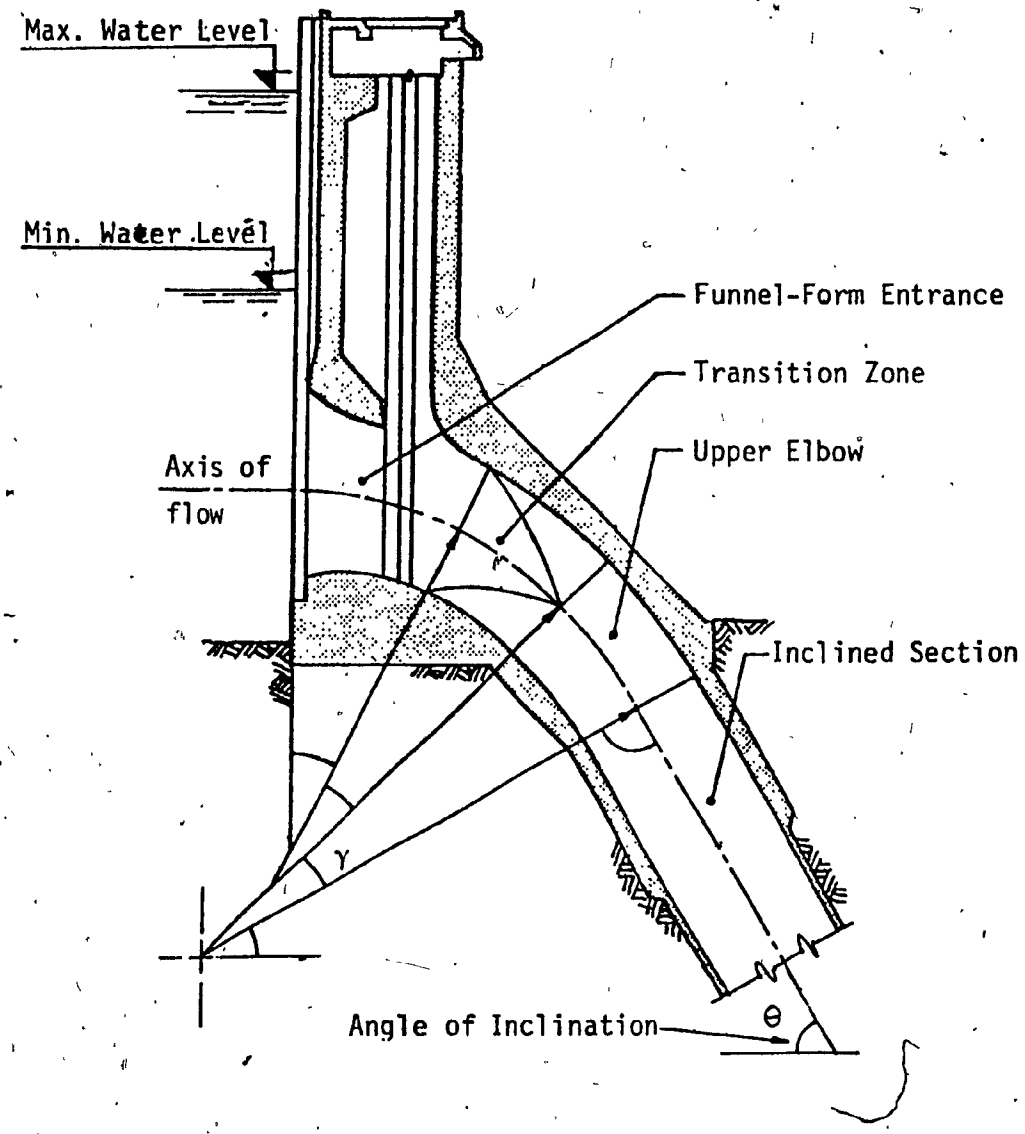

FIGURE 2.- Section through a water intake structure showing an upper elbow and an inclined section of the penstock.

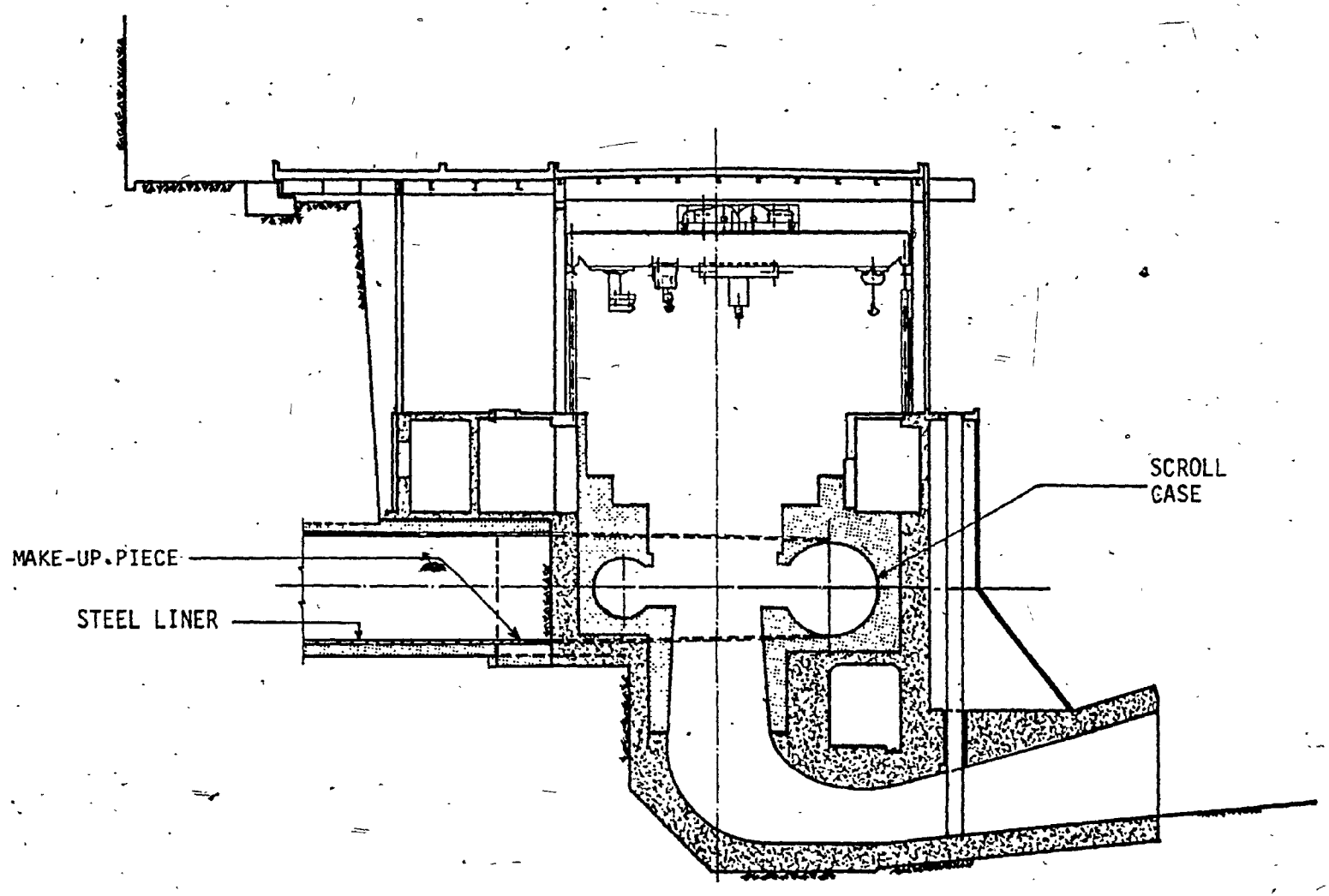

FIGURE 3.-Section through a penstock showing transition between the steel liner and the scroll case.

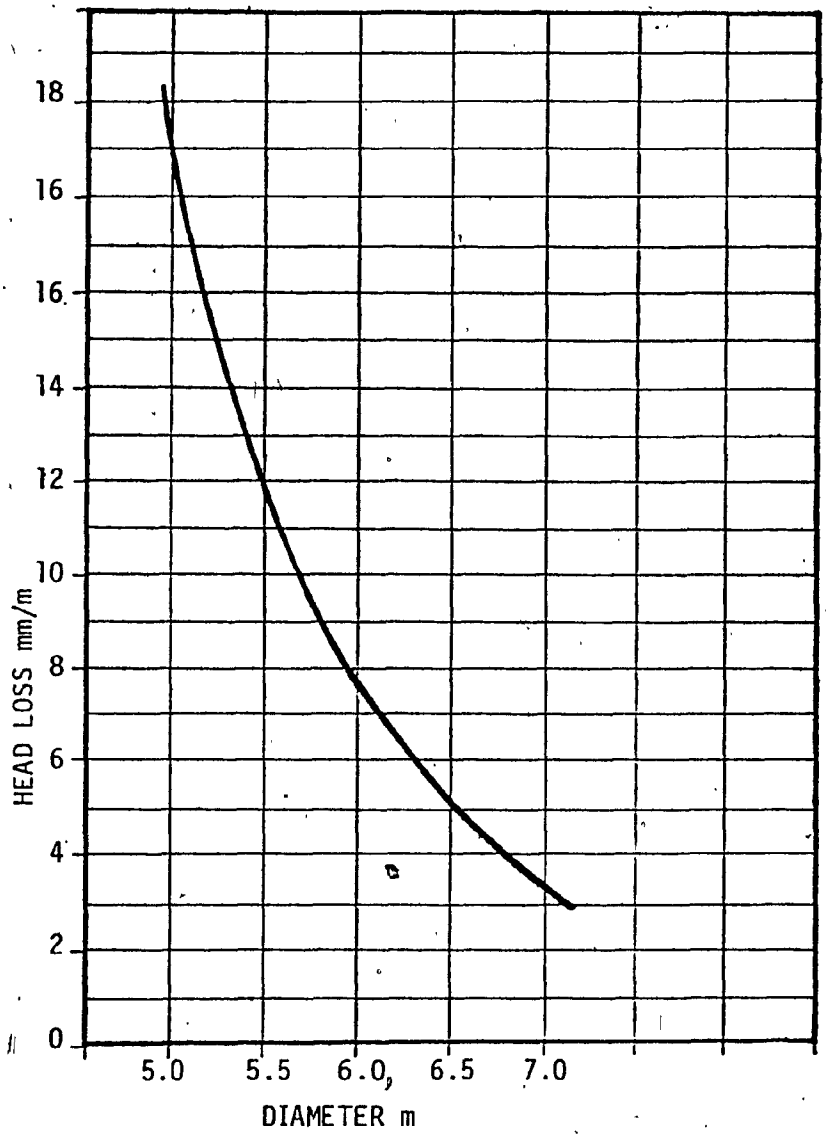

FIGURE 4.-Influence of change in diameter on head loss.

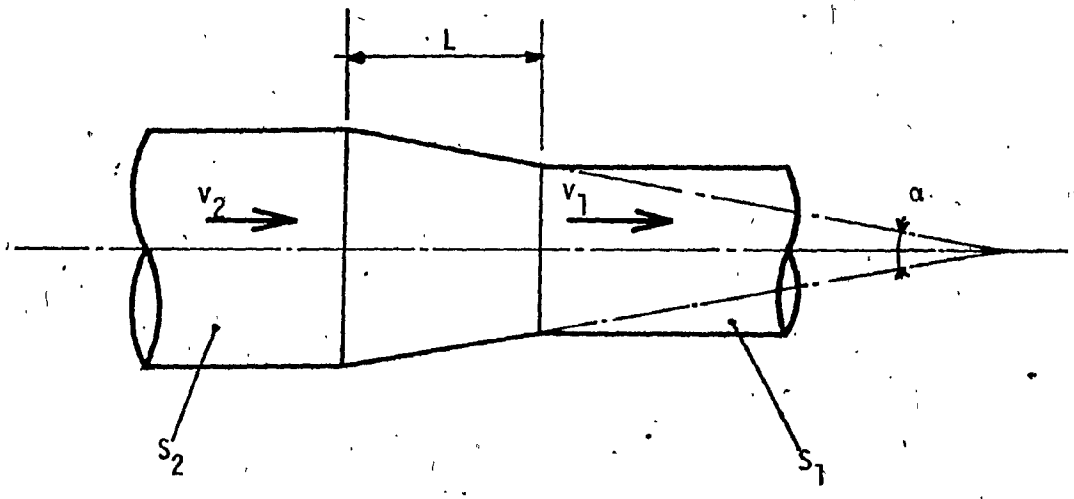

L=length of reducer

FIGURE 5.- Contraction in penstock diameter (reducer).

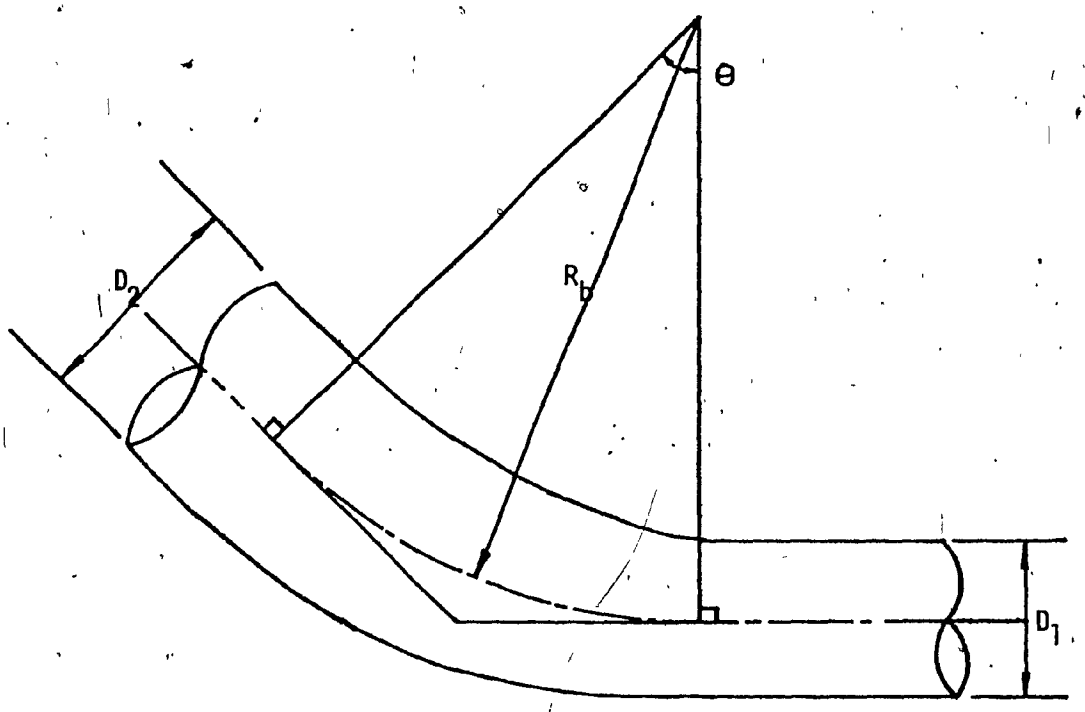

a) Reducer incorporated with the lower elbow of the penstock.

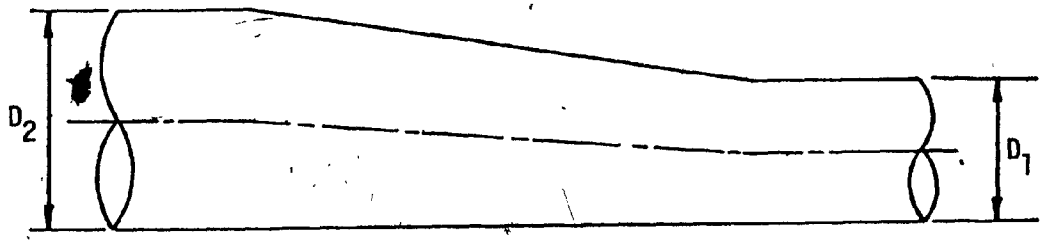

b) Reducer at downstream end of the horizontal concrete liner of the penstock.

FIGURE 6.- Two types of reducers.

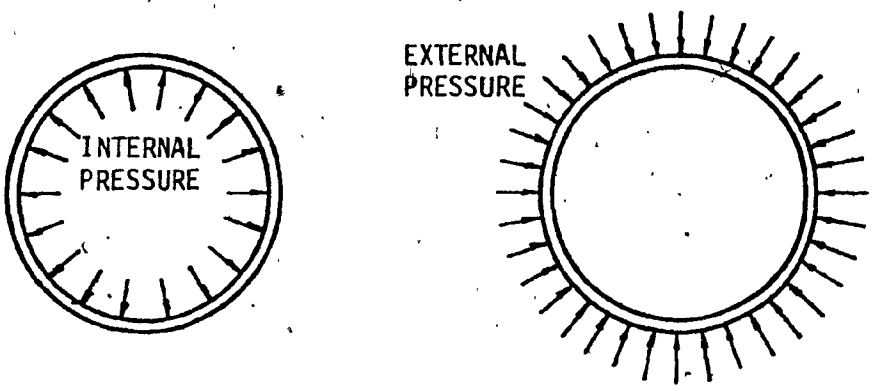

a) Liner with internal pressure loading

b) Liner with external pressure loading

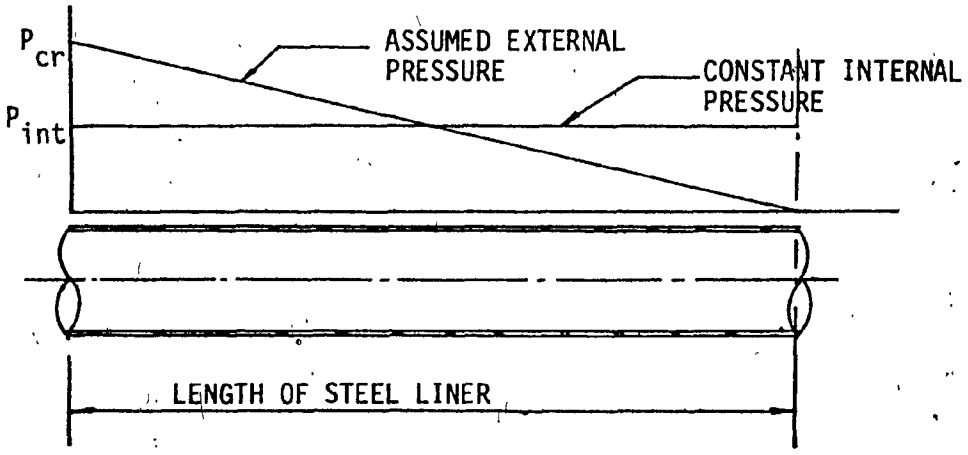

FIGURE 7.-Profile of a steel liner with internal and external pressures.

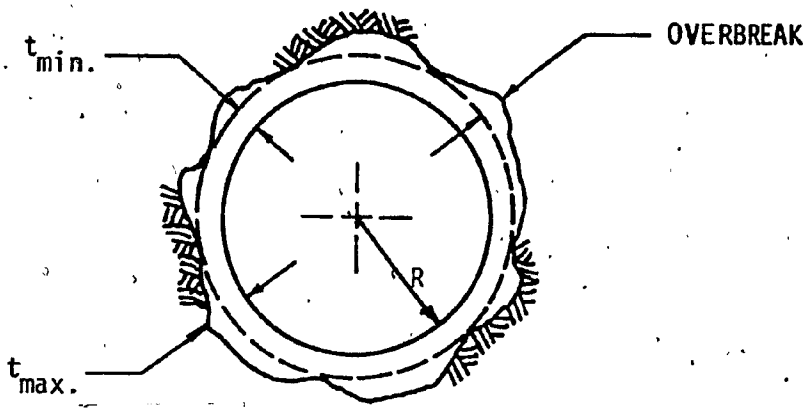

FIGURE 8.- Section through a concrete liner of the penstock.

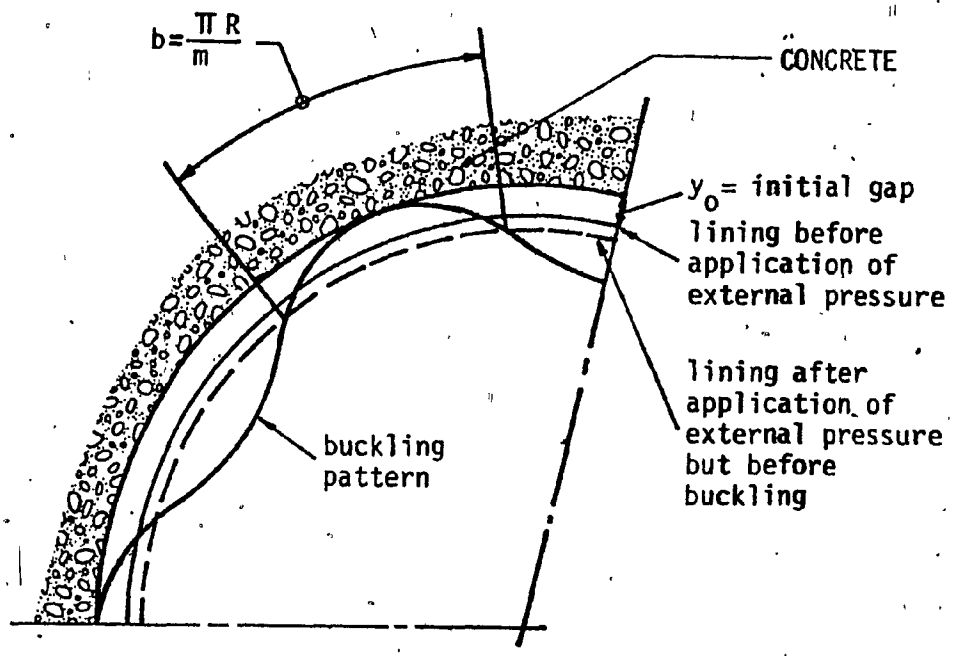

b = length of one half wave

$$M = \sqrt{\frac{3P_{cr}\,k^3}{2E'} + 1}$$

FIGURE 9.- Buckling according to Vaughan's theory.

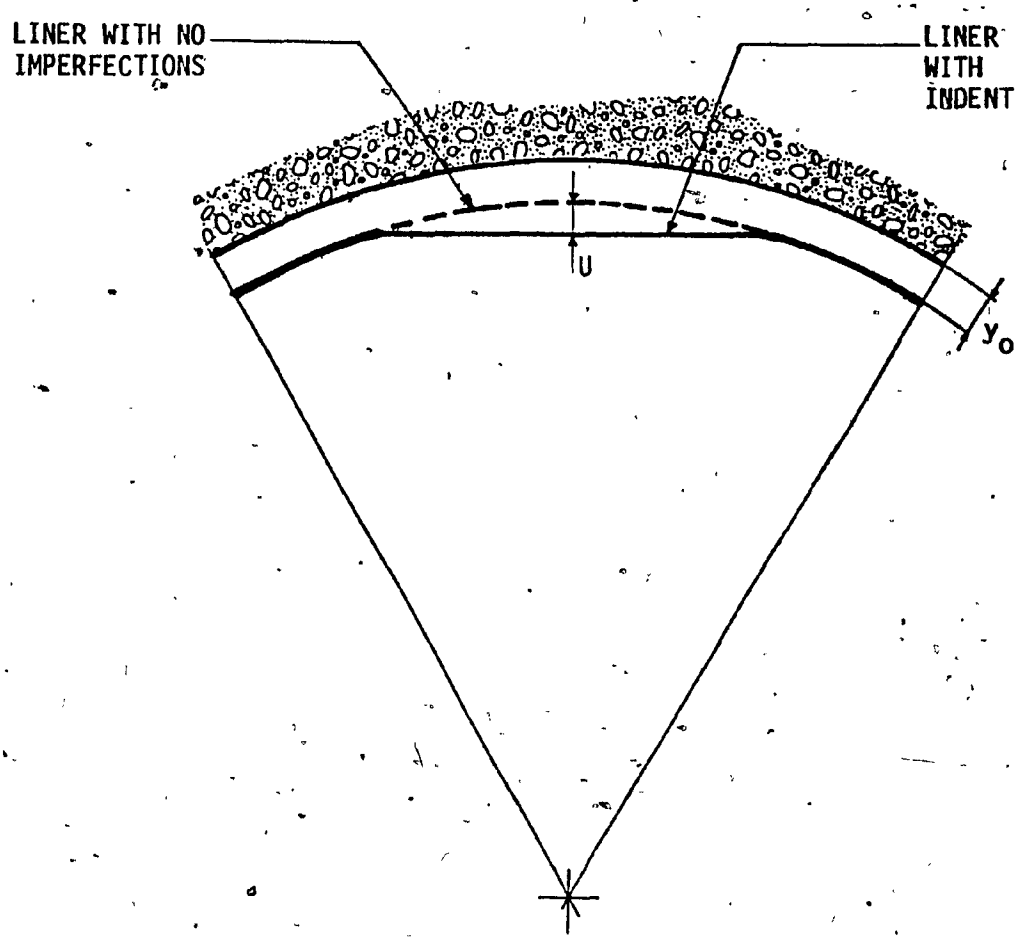

FIGURE 10.- Lining with initial imperfection (indent), taken into consideration in Montel's semi-empirical formula.

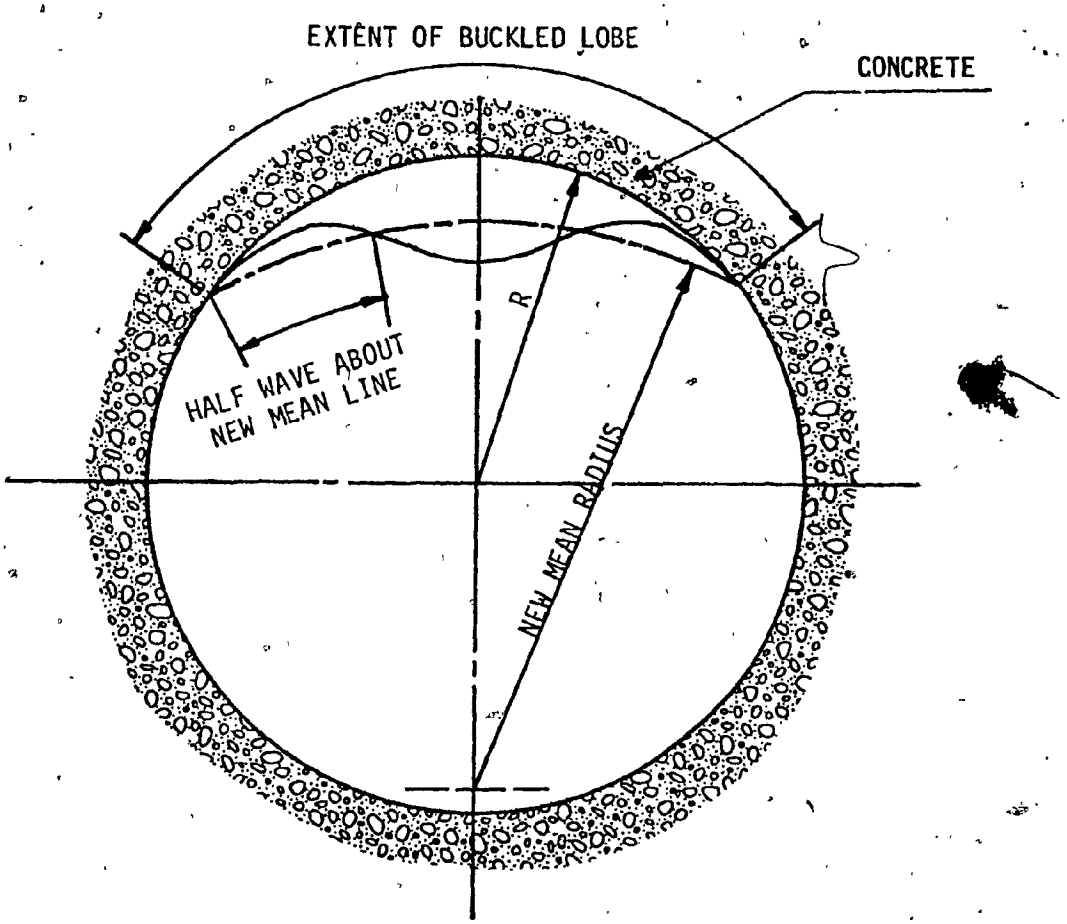

FIGURE 11.-Buckling according to Amstutz's theory.

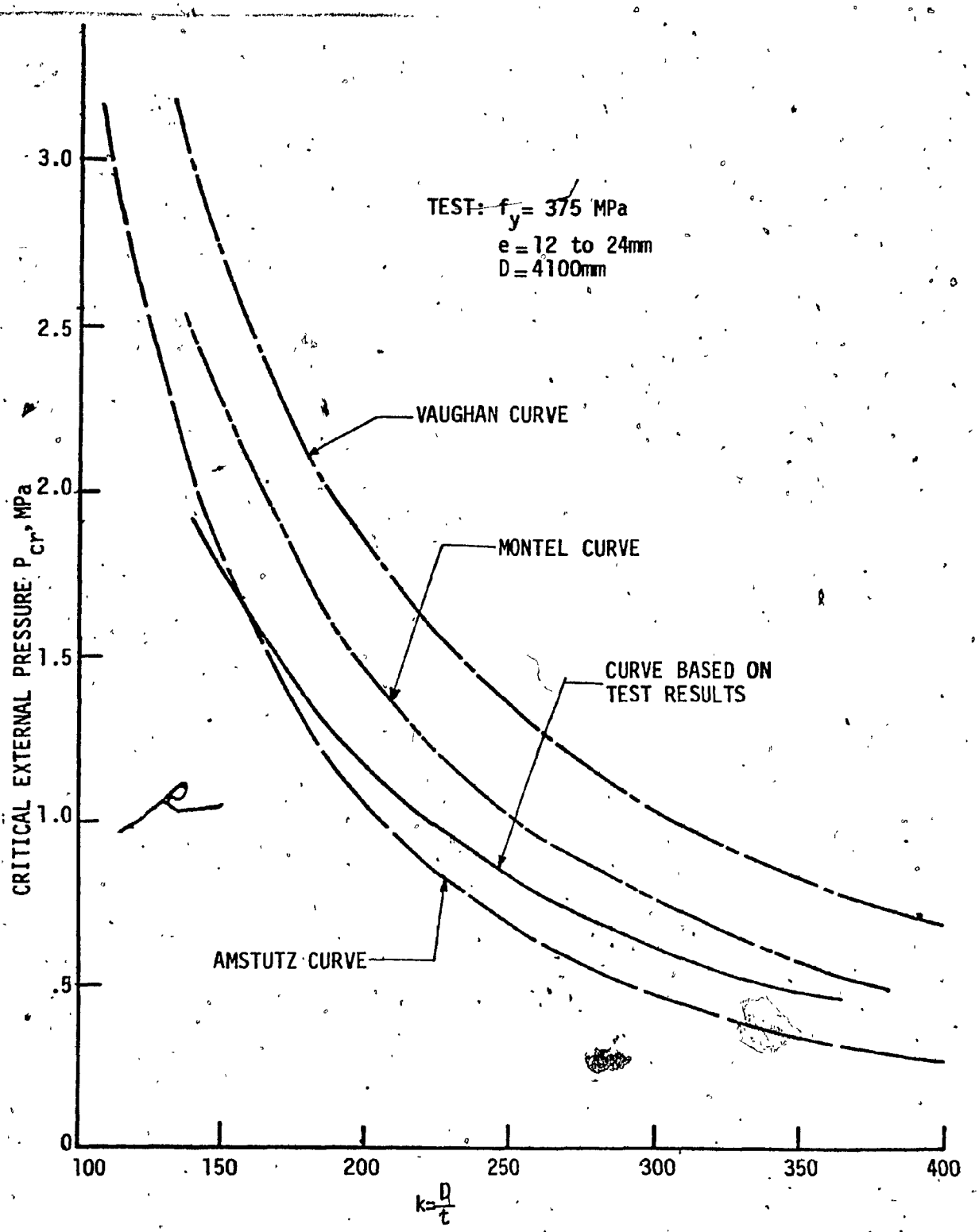

FIGURE 12.-Comparison of test results with theories.

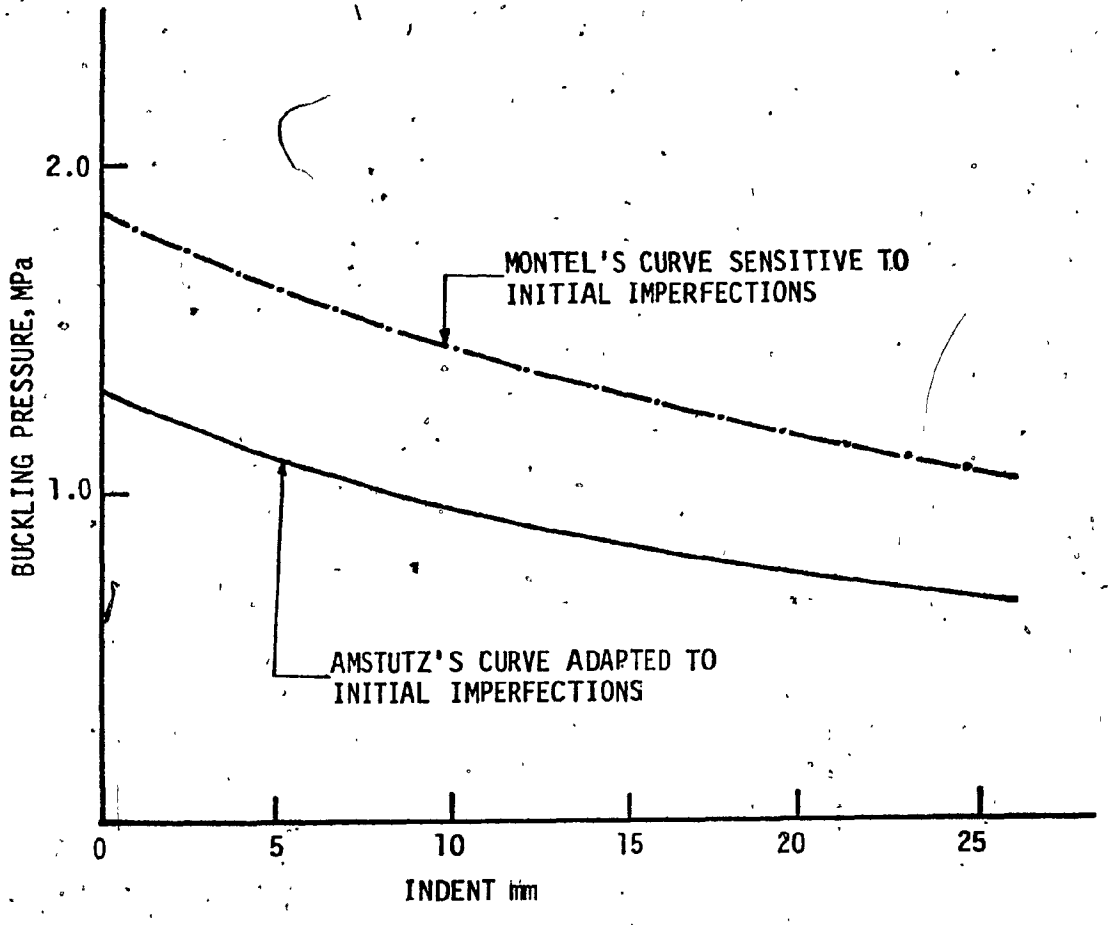

FIGURE 13.- Amstutz's curve adapted to initial imperfection in the steel liner according to the behavior of Montel's curve.

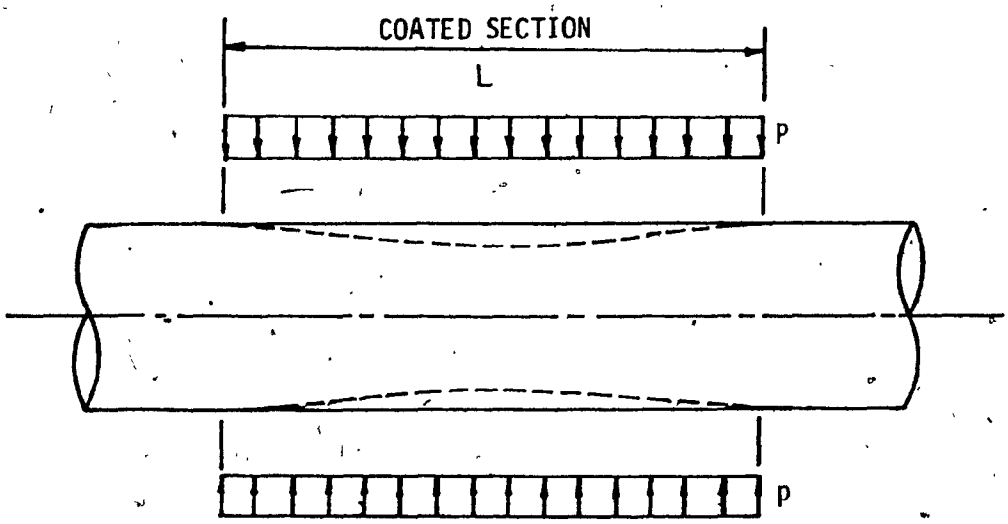

FIGURE 14.- Behavior of a partially oil coated steel liner under external pressure.

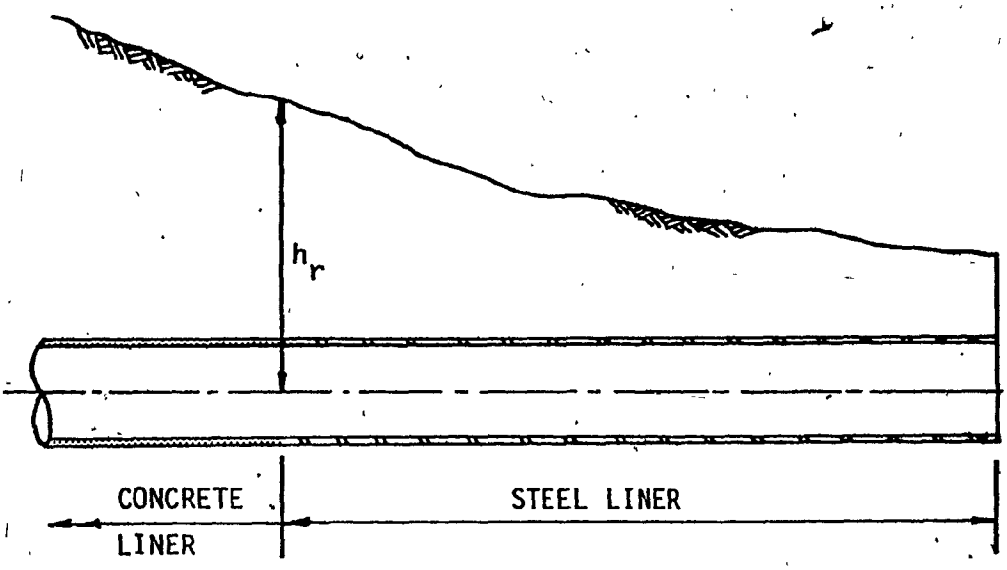

FIGURE 15.- Length of steel lined section according to Terzaghi.

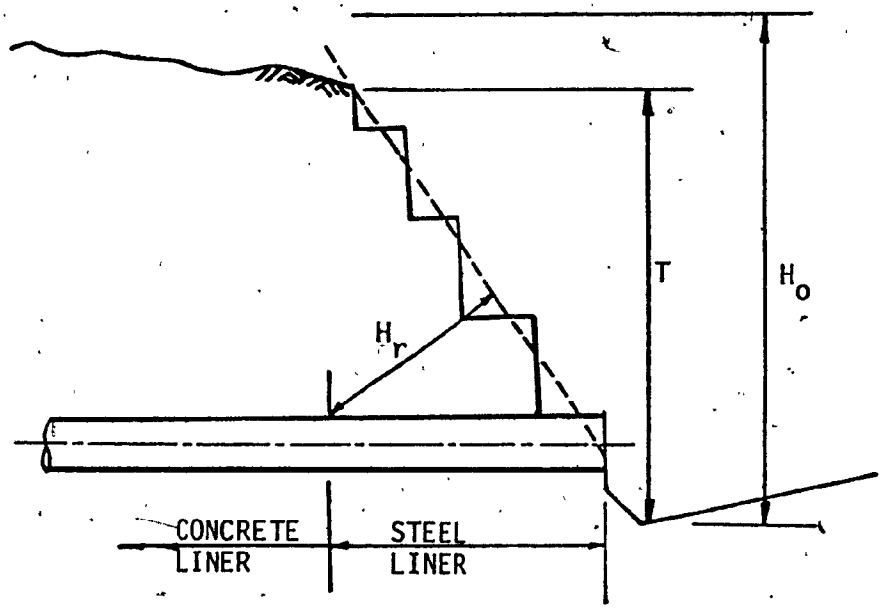

FIGURE 16.- Length of steel lined section according to Olsen.

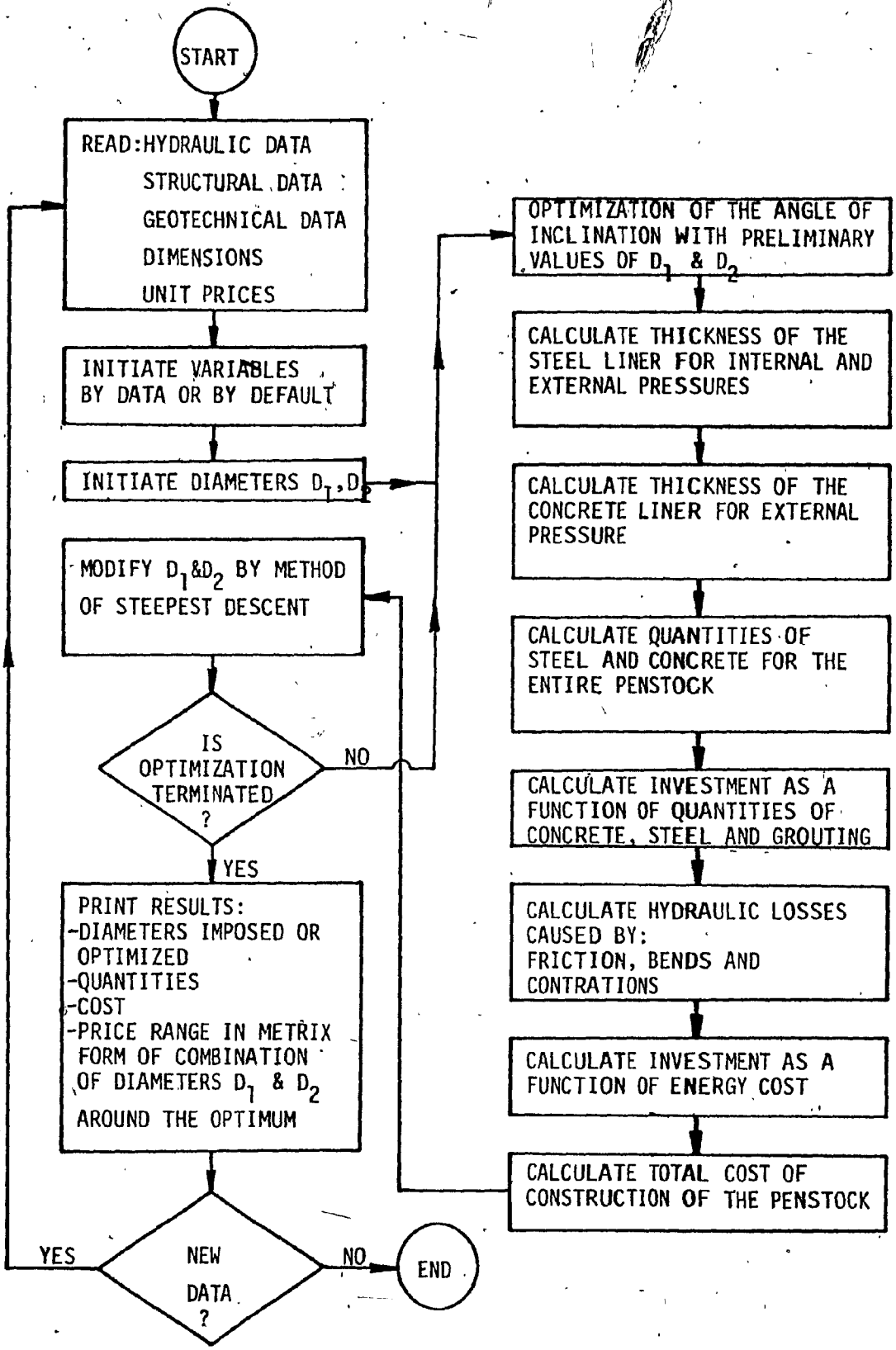

FIGURE 17.- Flowchart of the optimization procedure

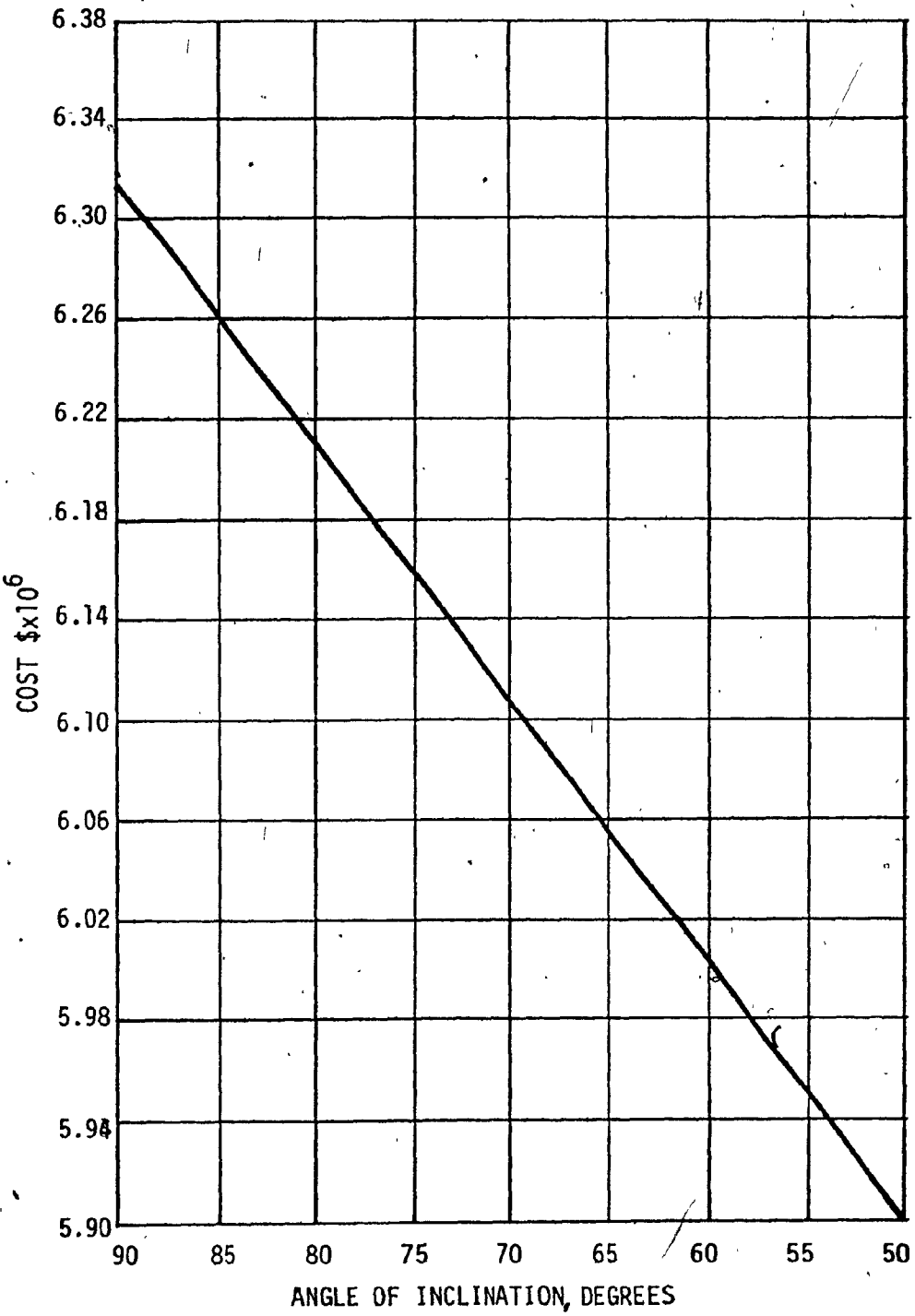

FIGURE 18.- Cost of construction of a penstock as a function of angle of inclination of the inclined section.

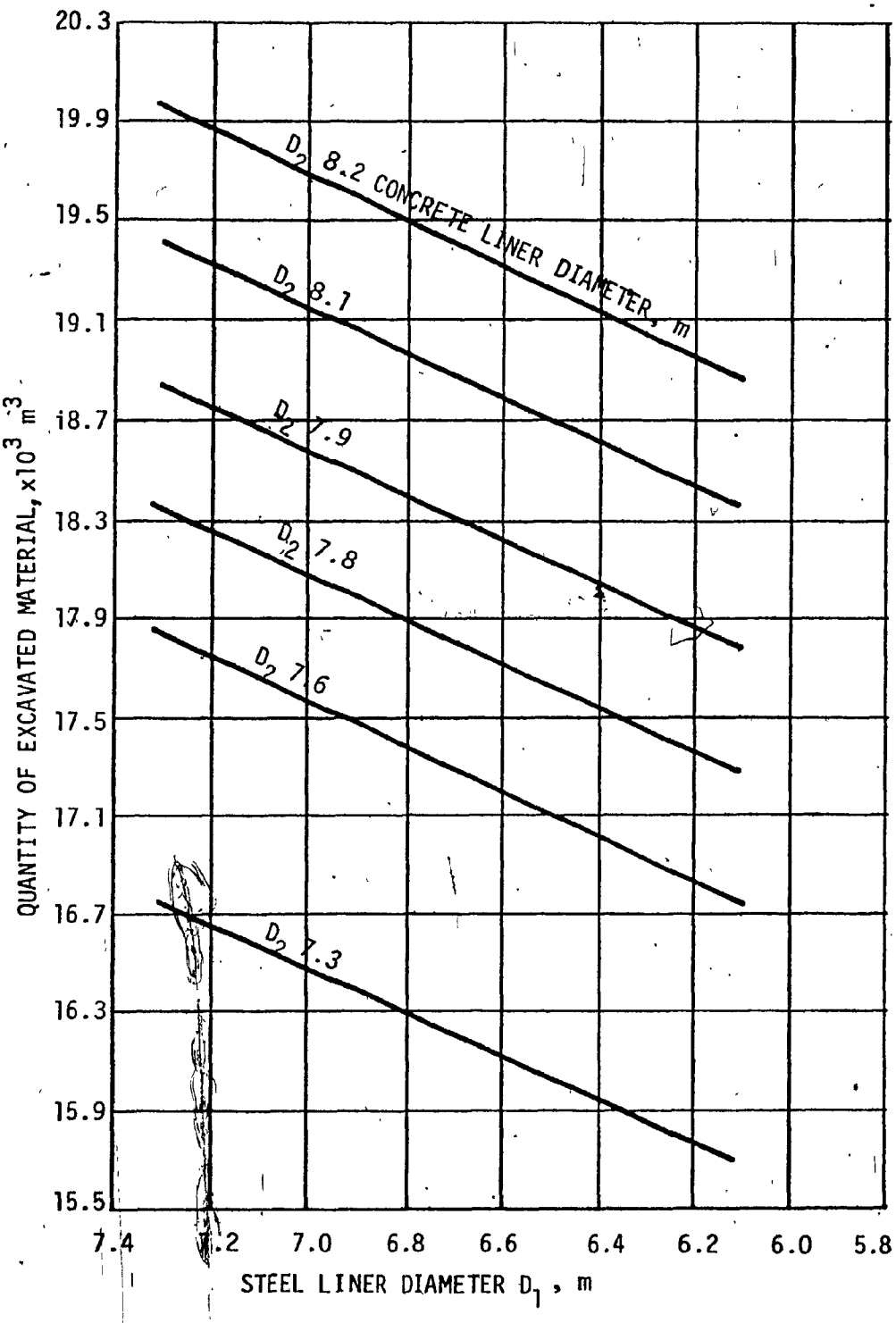

FIGURE 19.- Total excavation quantities for different combinations of diameters D_1 and D_2.

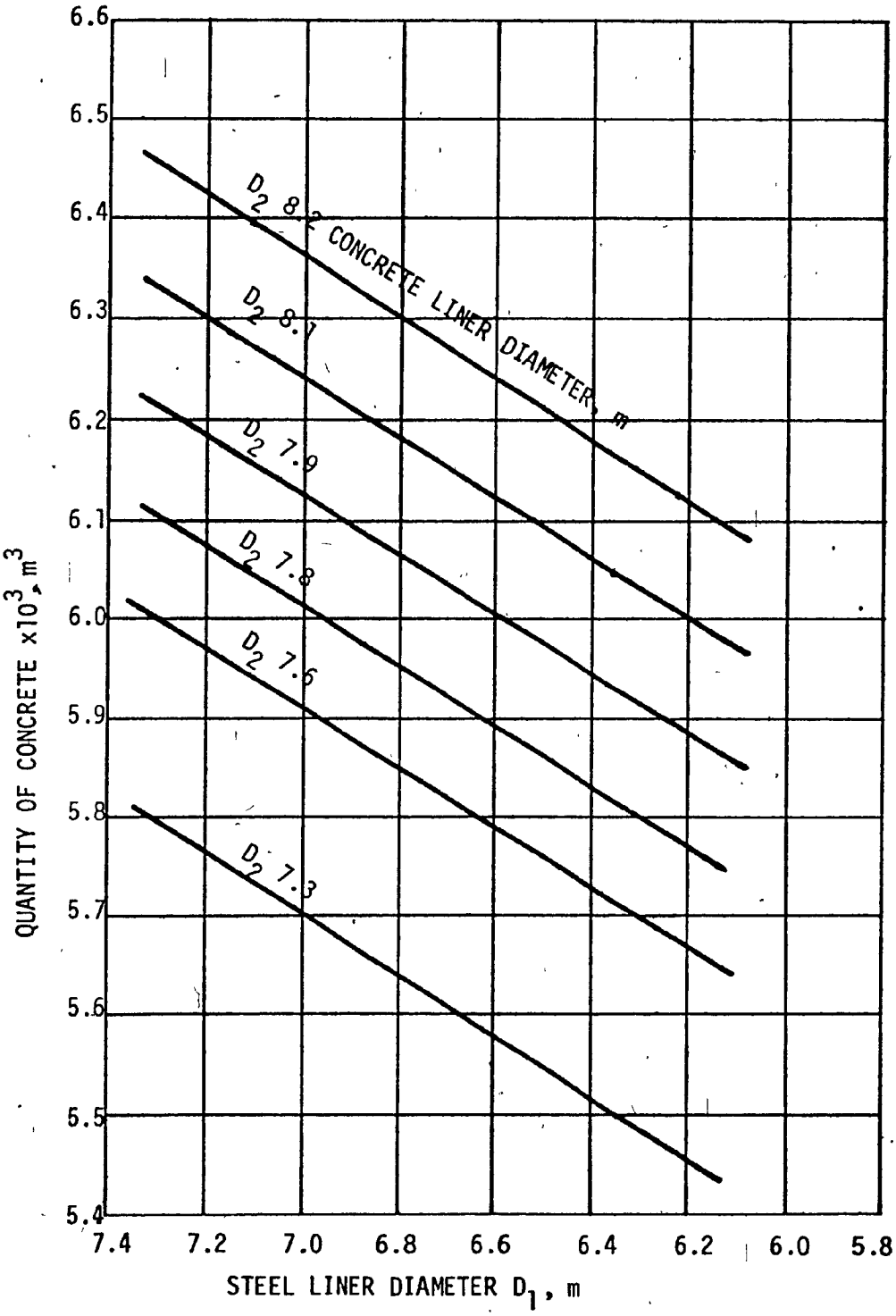

FIGURE 20.- Total concrete quantities for different combinations of diameters D_1 and D_2.

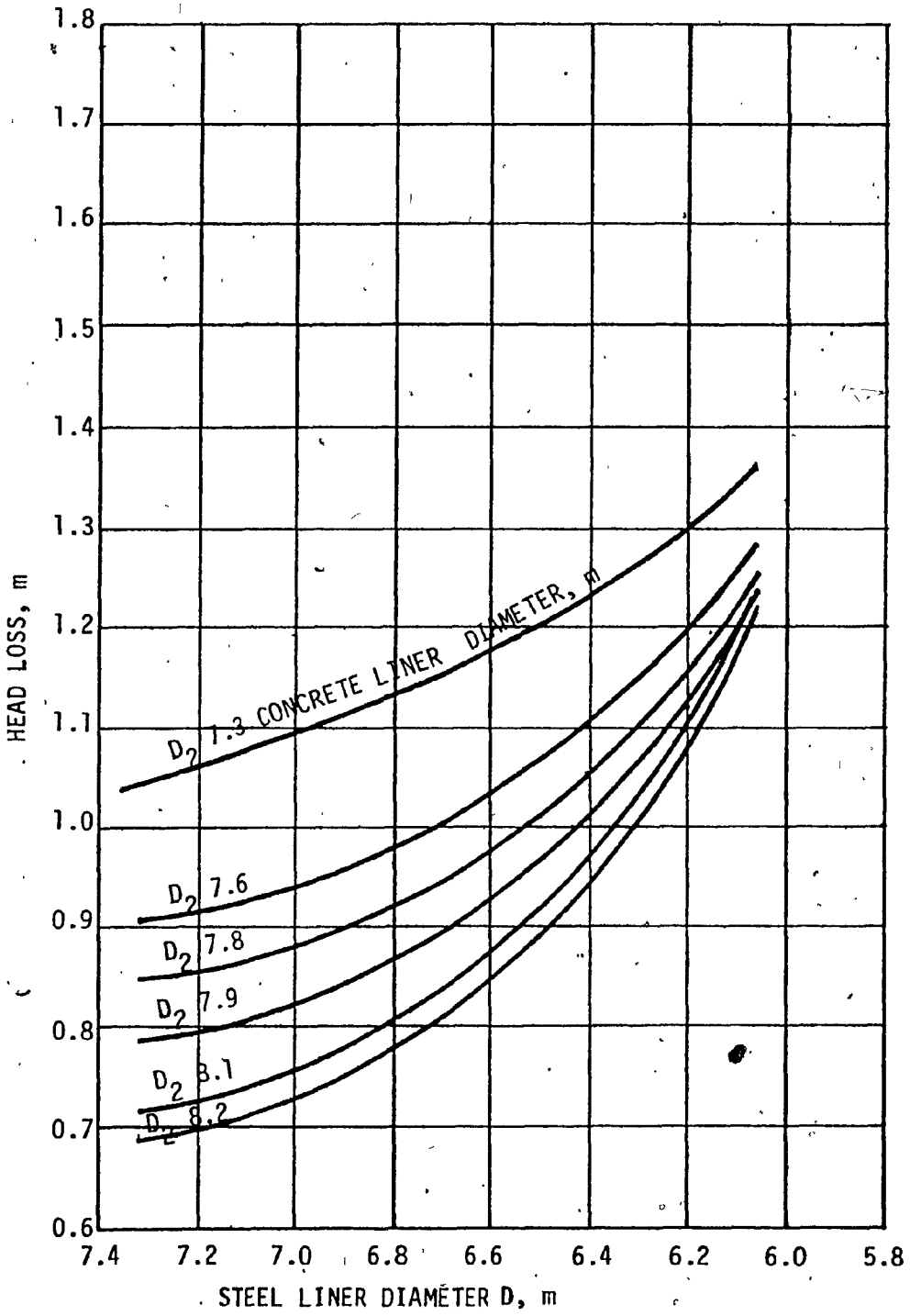

FIGURE 21.- Total head loss for different combinations of diameters D_1 and D_2.

D_1 \ D_2	7.32	7.47	7.62	7.77	7.92	8.07	8.23	8.38	8.53
7.62	6.23	6.15	6.10	6.06	6.04	6.03	6.04	6.06	6.09
7.47	6.19	6.12	6.06	6.02	6.00	6.00	6.01	6.03	6.07
7.32	6.16	6.08	6.03	5.99	5.97	5.97	5.99	6.02	6.07
7.16	6.13	6.05	6.00	5.97	5.95	5.96	5.98	6.02	6.07
7.01	6.10	6.03	5.98	5.96	5.95	5.96	5.99	6.04	6.10
6.86	6.09	6.02	5.98	5.96	5.96	5.98	6.02	6.08	6.15
6.71	6.09	6.02	5.99	5.98	5.99	6.02	6.07	6.14	6.23
6.55	6.10	6.04	6.02	6.02	6.04	6.09	6.16	6.24	6.34
6.40	6.13	6.09	6.08	6.09	6.13	6.20	6.28	6.38	6.50
6.25	6.19	6.17	6.17	6.20	6.26	6.34	6.45	6.57	6.71
6.10	6.29	6.28	6.31	6.36	6.44	6.55	6.67	6.82	6.99

FIGURE 22 - Matrix of a concave upward surface formed by costs of diameters D_1 and D_2

APPENDIX A

TABLE 1 - Rugosity for Large Penstocks

Material	Condition	Size (ε) 10^{-2},mm
Concrete	Unusually rough; poor alignment at joints	90 - 60
	Rough; visible form marks spalling	60 - 35
	Wood-floated or brushed surface in good condition; good joints	35 - 20
	Centrifugally cast; new; smooth; steel forms	20 - 15
	Average workmanship; smooth joints; new; very smooth; steel forms	18 - 6
	First-class workmanship; smooth joints	6 - 2
Butt-welded steel	Severe tuberculation and incrustation	610 - 245
	General tuberculation	245 - 95
	Heavy brush-coated enamels and tars	95 - 35
	Light rust	35 - 15
	Hot-asphalt-dipped	15 - 6
	New smooth pipe; centrifugally applied enamels	6 - 0.9
Corrugated metal	Depth of corrugation 12 mm Spacing of corrugations 75 mm	4570 - 5485
Rock	Unlined	61000

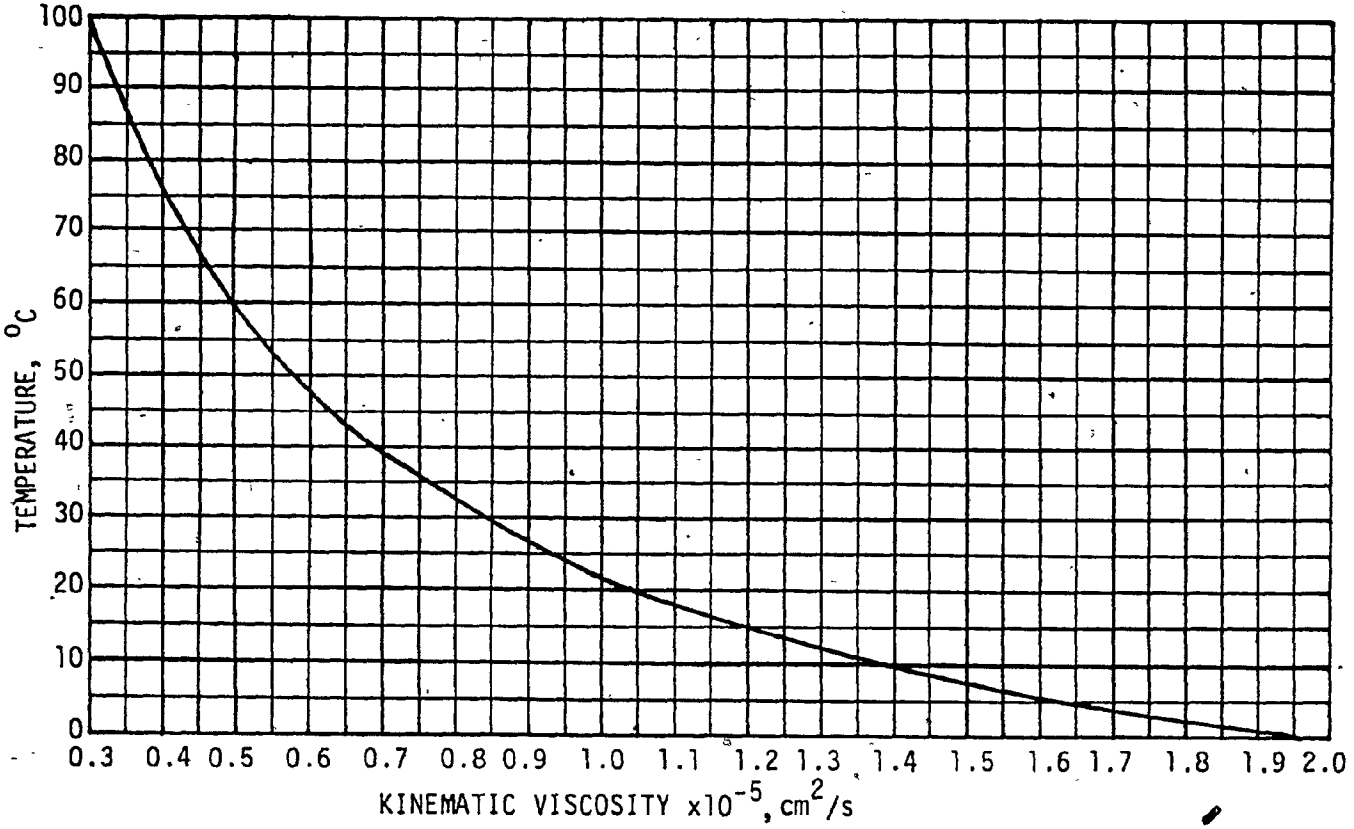

CHART 1.- Values of kinematic viscosity ν_k of water as a function of temperature

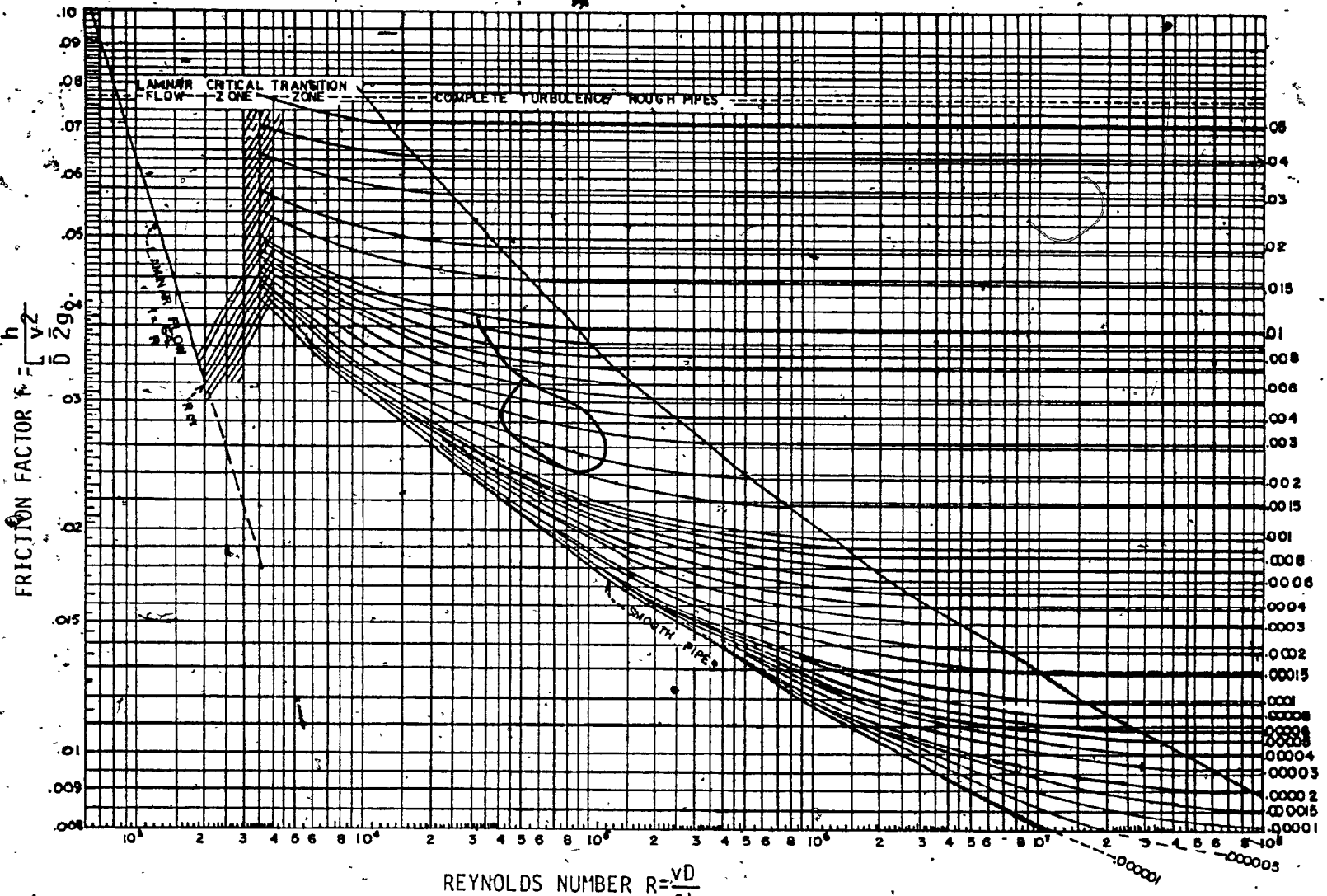

CHART 2:- Moody's diagram for friction factors. $\frac{k}{}$

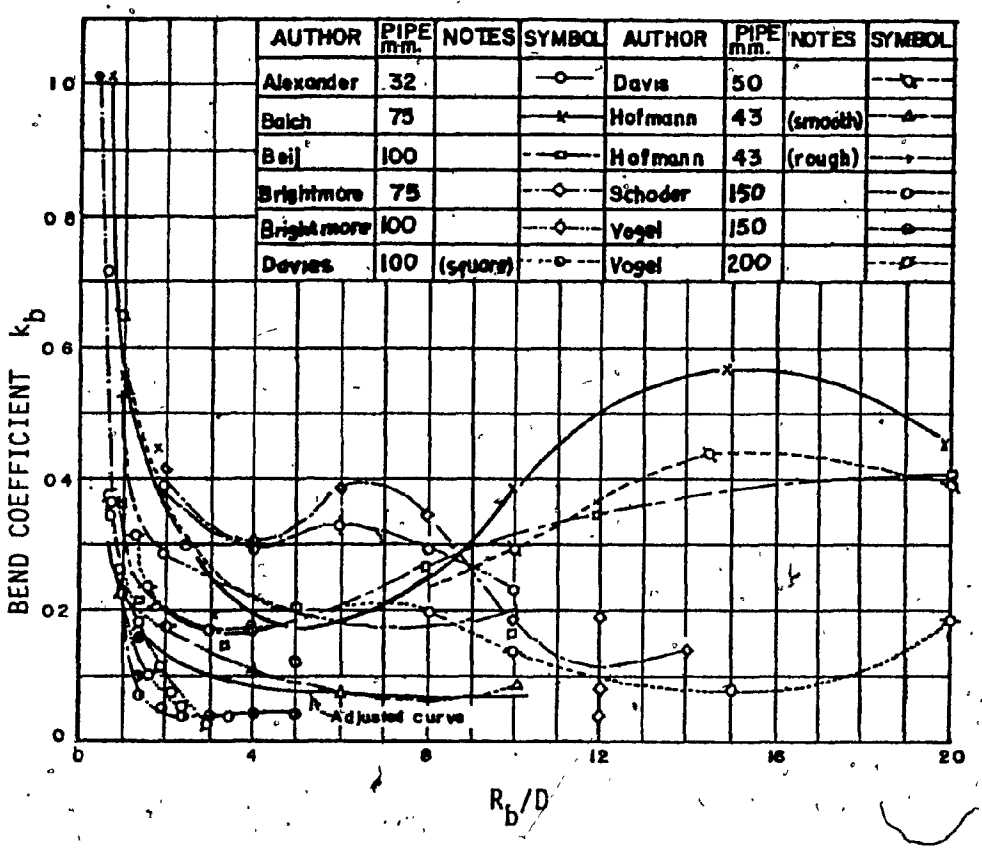

CHART 3.- Bend factors for small diameter conduits.

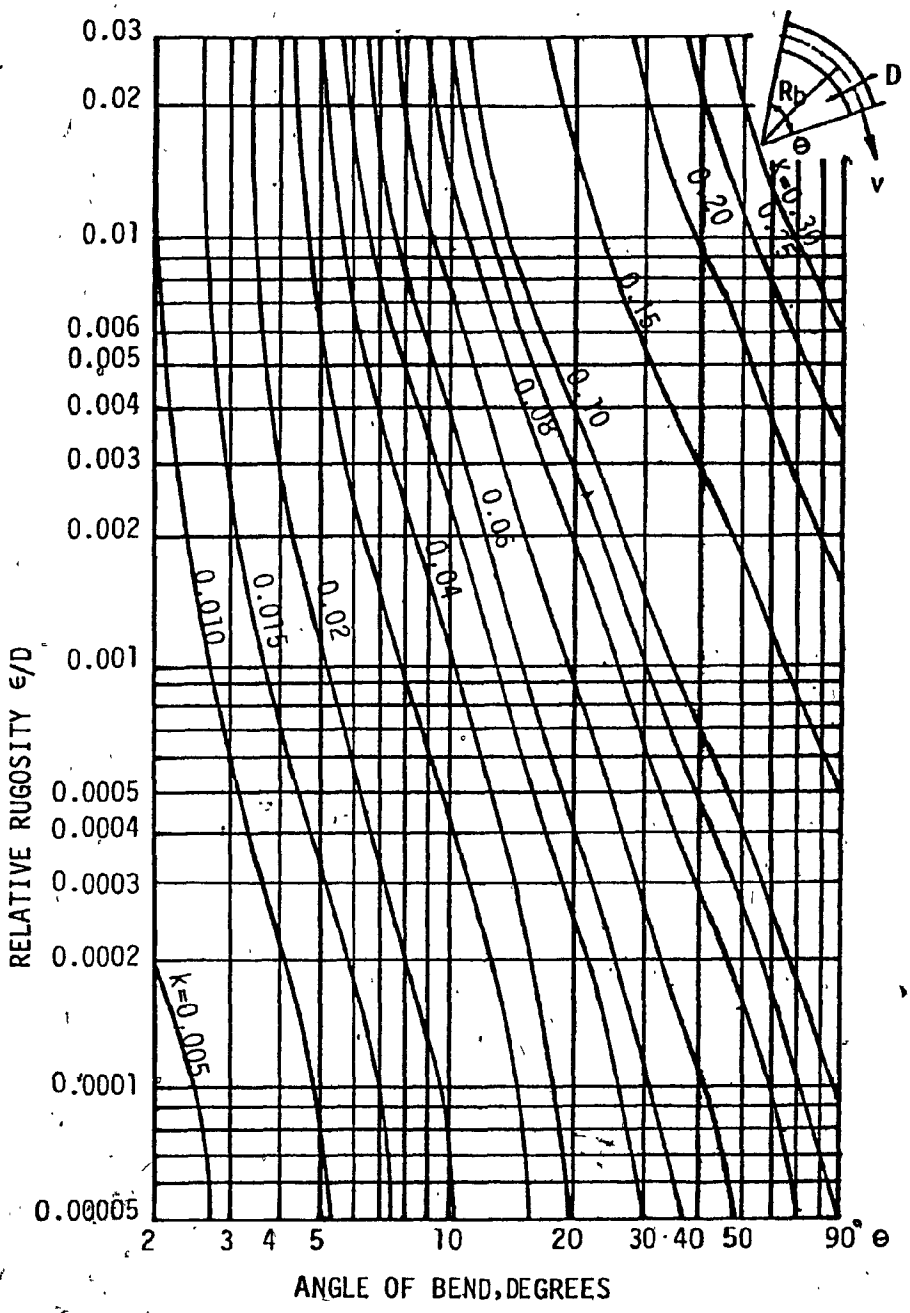

CHART 4.- Bend factors as a function of bend angles for $R_b/D=10$

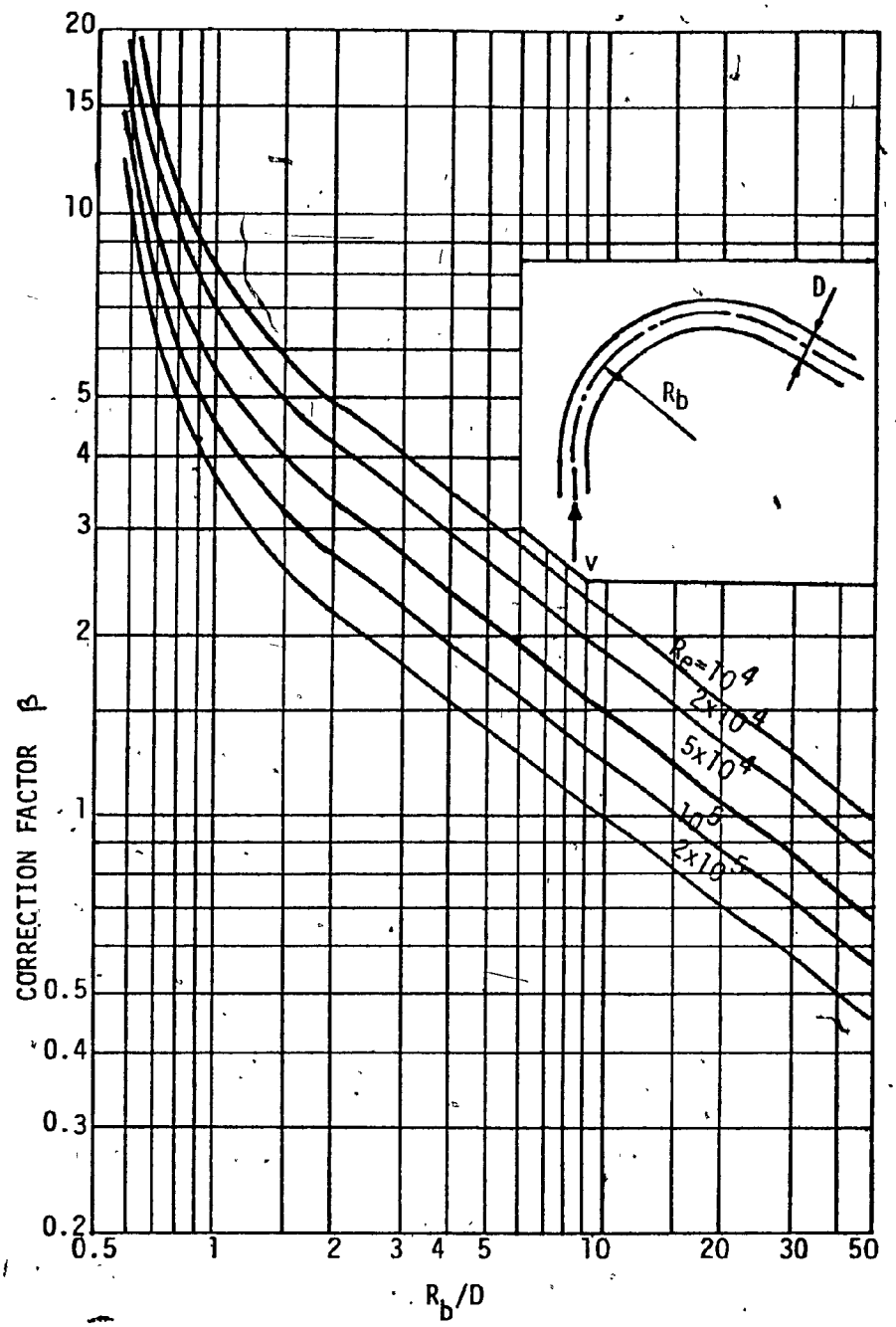

CHART 5.- Correction factors for $R_b/D \neq 10$.

APPENDIX B

Bending of an Axisymmetrically Loaded Cylindrical Shell

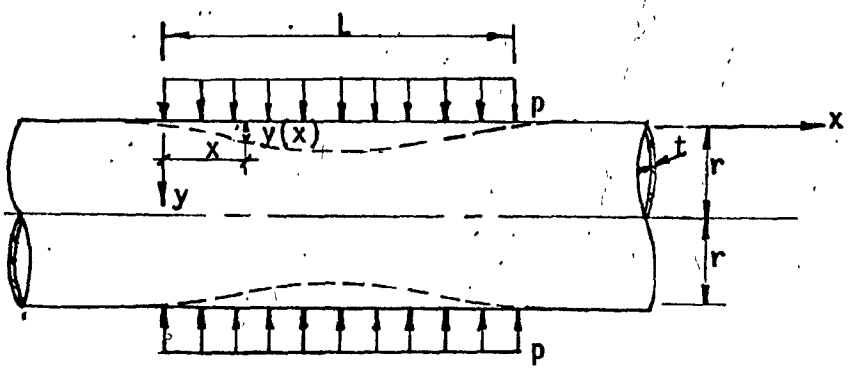

Solution for deflection of a pipe under ring load P is found to be (16):

$$y(x) = \frac{P}{8\beta^2 D}\phi(\beta x) \qquad (B1)$$

Where: $\phi = e^{-\beta x}(\cos \beta x + \sin \beta x)$;

$$\beta^4 = \frac{3(1-\nu^2)}{r^2 t^2} \; ;$$

$$D = \frac{Et^3}{12(1-\nu^2)}$$

Integrating B1 in case of distributed load for P = p.dx over the length, L :

$$y(x) = \frac{p}{8\beta^4 D}\left[2 - \theta(\beta(L-x)) - \theta(\beta x)\right] \qquad (B2)$$

and

$$M(x) = \frac{p}{4\beta^2}\left[\rho(\beta(L-x)) + \rho(\beta x)\right] \qquad (B3)$$

Where: $\theta(z) = e^{-\beta z}\cos \beta z$;

$\rho(z) = e^{-\beta z}\sin \beta z$

For maximum bending moment ; $x = L/2$

$$M_{max} = \frac{P}{2\beta^2} \cdot e^{-\beta L/2} \cdot \sin \beta L/2 \qquad (B4)$$